ISSN 0280–5316
ISRN LUTFD2/TFRT 5718 SE

Untripped SUV Rollover Detection and Prevention

Björn Johansson

Department of Automatic Control
Lund Institute of Technology
February 2004

Department of Automatic Control
Lund Institute of Technology
Box 118
SE 221 00 Lund Sweden

Document name
MASTER THESIS

Date of issue
February 17, 2004

Document Number
ISRN LUTFD2/TFRT 5718 SE

Author(s)
Björn Johansson

Supervisor
Prof. Anders Rantzer
Dr. Magnus Gäfvert

Sponsoring organisation

Title and subtitle
Untripped SUV Rollover Detection and Prevention (Vältskydd för SUVs)

Abstract

Untripped SUV (Sport Utility Vehicle) rollovers are dangerous and possibly lethal accidents. This thesis address some issues in the detection and prevention of untripped SUV rollovers.

Before a rollover can occur, the wheels on one side must lose road contact. The wheel lift off situation is chosen as the critical situation to be avoided. If wheel lift off is prevented, then rollover is prevented as well.

A new kinetic energy based measure, that indicates an imminent wheel lift off, is introduced. This measure is used by a gain scheduled LQ (Linear Quadratic) controller to prevent wheel lift off. The LQ controller outputs the desired changes of the forces acting on the chassis. These force changes are mapped to braking and traction system commands by a control allocator. Three different control allocation approaches were evaluated, including a new convex optimization approach. The convex optimization approach seems to work well. The controller is capable of preventing wheel lift off in the simulated test cases, and the results are promising.

Key words
rollover, sport utility vehicle, vehicle dynamics, control allocation, convex optimization

Classification system and/ or index terms (if any)

Supplementary bibliographical information

ISSN and key title
0280–5316

ISBN

Language
English

Number of pages
58

Recipient's notes

Security classification

Acknowledgment

Thanks everybody! Especially, I would like to thank Prof. Anders Rantzer and Dr. Magnus Gäfvert for excellent supervision and guidance.

Lund, 17th February 2004

Björn Johansson

Contents

List of Figures

1. Introduction

Rollover occurs when a car flips over, see Figure 1.1. There are two types of rollover, tripped and untripped. Tripped rollover is the most common type, and occurs when the car has started to skid, hits an obstacle, and finally flips over. Untripped rollover is induced by the driver, either intentionally during extreme maneuvers, or unintentionally in panic situations (Oden thal et al. 1999).

Rollover is the second most dangerous car crash on American Highways. The year 2000, 9,882 people were killed in light vehicle rollover crashes, including 8,146 killed in single vehicle rollovers. Vehicles with high centers of gravity (center of gravity is hereafter denoted CG), e.g., Sport Utility Vehicles, SUVs, are becoming more and more popular. These vehicles are more likely to rollover during extreme maneuvers compared to ordinary cars (Forkenbrock et al. 2003). The tripped rollover is well understood, and it is responsible for the majority of the fatalities. The untripped rollover is not well understood, and it is only responsible for a small portion of the fatalities (Howe et al. 2001). Still, people are getting killed by untripped rollovers, and research on this subject is motivated. Tripped rollovers can be avoided if a control system prevents the vehicle from uncontrolled skidding, e.g., Electronic Stability Program, ESP (van Zanten et al. 1996). Untripped rollovers can be avoided if a control system lets the vehicle deviate from the nominal trajectory. The aim for this work is to find a control system that can prevent untripped rollovers, with minimum trajectory deviation.

The controller will use the brakes and the traction system as actuators. Controllable brakes are standard on many cars, and they are therefore cheaper and more available compared to other actuators. Traction systems that can distribute driving torque between the different wheels are not that easily available, but will provide more freedom for the controller.

Vehicle control is an active research field, both in the academic world and in the car industry, and much effort is spent on finding better and better solutions. However, due to financial reasons, much information is proprietary. This makes it difficult to get to know what others have done and how they did it.

Figure 1.1 SUV in the beginning of a rollover.

1.1 Objectives and Approach

The objectives of the thesis can be structured in the following way.

- Prevent untripped rollovers.
- Minimize the deviation from the nominal (desired) trajectory.

The problem has been divided into five smaller problems.

- Investigate the underlying physics of cars and tires.
- Construct vehicle model and implement it in Simulink.
- Find a measure that indicates a potential rollover.
- Design a controller that uses the measure above to achieve the objec tives.
- Design a control allocator that distributes the desired control action between the four wheels.

Scope

In order for the controller to work properly, it is essential to know the states of the vehicle. In automatic control this is accomplished with an *observer*. The observer is very important, but it is outside the scope of this thesis. It is also necessary to know the parameters of the vehicle, but this is also outside the scope of this thesis. Thus, it is assumed that all states and vehicle parameters are known.

Outline

The thesis outline is as follows. First the basic concepts, terminology, and the used mathematical models are introduced. This is followed by a chap ter on a new rollover measure. This measure is then used in the controller design. The rollover measure and the controller are tested in simulations, and the results are discussed. Finally, suggestions on future work are pre sented.

Software

Matlab[1] and Simulink[1] were used for simulation and model implementa tion. This text was produced with LaTeX[2]. The optimization was performed with SeDuMi[3], using the parser YALMIP[4].

[1] http://www.mathworks.com/
[2] http://www.latex-project.org/
[3] http://fewcal.kub.nl/sturm/software/sedumi.html/
[4] http://www.control.isy.liu.se/~johanl/yalmip.html/

2. Background

In order to prevent rollover, it is crucial to have an accurate vehicle dy namics model. The primary source of the forces acting on the vehicle is the road. The forces are developed in the contact patches between the tires and the road. Thus, a good understanding is needed of how the chassis reacts on external forces, and of the tire ground behavior (Wong 2001).

To simplify the equations of motion, a coordinate system attached to the vehicle is used (see Figure 2.1). X and Y represent an inertial system, and x and y represent a moving axes system that is attached to the vehicle. The x axis is parallel with the vehicle heading. Take special note that this differs from the standard natural coordinates, where the x axis is parallel with the trajectory. When the equations of motion are introduced later in the text, the yaw angle rate, r, is used as a state variable instead of the yaw angle, Ψ, i.e., $r = \dot{\Psi}$. The vehicle velocity is often divided into two components, one parallel with the x axis, $V_x = u$, and the other one parallel with the y axis, $V_y = v$. The vehicle acceleration is also often divided into components as above, a_x, and a_y. The relationship between them is derived by differentiation, which yields (Wong 2001):

$$\begin{aligned} a_x &= \dot{u} - vr \\ a_y &= \dot{v} + ur \end{aligned} \tag{2.1}$$

2.1 Models

The characteristics of the tires are important. In order for the tires to produce lateral forces, they need to slip sideways. In the simplest model, the lateral force is considered to depend linearly on the slip angle. This neglects the fact that the tire forces saturate. Two models will be used: a simple linear model, and a non linear model incorporating the saturation property.

The characteristics of the chassis are also important. The most com mon model used in control design is the bicycle model. This is a model that considers planar motions only, but since the goal in this work, is to mini mize roll, it is not sufficient for simulation and design. However, the linear model will be used to provide the nominal trajectory to the controller. A more advanced model is needed for simulation and controller design. The hard issue is to select a model that is simple enough to be manageable and

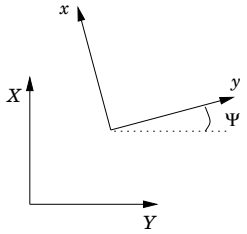

Figure 2.1 The coordinate system.

complex enough to capture the essential characteristics. Two chassis mod els are used, the linear bicycle model mentioned and a non linear model with roll movement.

Tires

The forces, which the driver can influence, are induced by the tires. A tire needs to slip to produce forces. It can slip in two directions, laterally and longitudinally. There exist two slip quantities to describe the two different slips:

- The slip angle or tire slip angle, α, corresponding to lateral slip.
- The longitudinal slip, κ.

The slip angle is defined as:

$$\tan(\alpha) = -\frac{V_{y_{Tire}}}{V_{x_{Tire}}} \Rightarrow \alpha \approx -\frac{V_{y_{Tire}}}{V_{x_{Tire}}} \tag{2.2}$$

where $V_{x_{Tire}}$ and $V_{y_{Tire}}$ corresponds to the longitudinal velocity and lateral velocity in a coordinate system attached to the tire, see Figure 2.2. The longitudinal slip is defined as:

$$\kappa = -\frac{\Omega_0 - \Omega}{\Omega} \tag{2.3}$$

where Ω_0 is the angular speed of the freely rolling wheel, and Ω is the angular speed of the braked or accelerated wheel.

Lateral slip occurs when the velocity of the tire is different from the heading of the tire. This can be caused by the steering angle ($|\delta| > 0$) and/or the yaw rate ($|r| > 0$), e.g., during cornering. Longitudinal slip occurs when a driving or braking torque is applied to the wheel, e.g., during braking.

Another slip quantity is also needed, the vehicle side slip angle or side slip angle, β, which is defined as:

$$\tan(\beta) = -\frac{V_{y_{Vehicle}}}{V_{x_{Vehicle}}} = -\frac{v}{u} \Rightarrow \beta \approx -\frac{v}{u} \tag{2.4}$$

A normal car has four wheels, which implies that there will be four tire slip angles, one for each tire. To simplify the analysis, it is usually assumed that the front wheels have the same slip angle (denoted α_F or α_1), and that the rear wheels have the same slip angle (denoted α_R or α_2). Naturally, there is only one vehicle side slip angle. The tire slip angle and the vehicle side slip angle are visualized in Figure 2.2.

In general, the longitudinal and lateral forces are dependent on three variables, $F_x = F_x(\kappa, \alpha, F_z)$ and $F_y = F_y(\kappa, \alpha, F_z)$, where κ is the longi tudinal slip, α is the slip angle, and F_z is the vertical normal force. The tire forces do also depend on the angle between the wheel plane and the XZ plane, the camber angle, γ. To simplify the models, this dependence has been neglected (Pacejka 2002).

Figure 2.2 *Left* The tire slip angle. The rectangle illustrates the tire. *Right* The vehicle side slip angle. The rectangle illustrates the vehicle. Note the difference in scale.

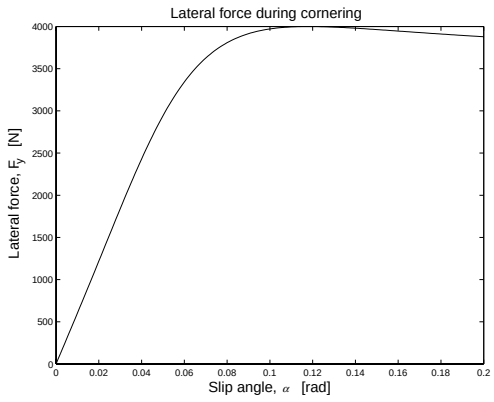

Figure 2.3 Lateral force during cornering.

Linear Model The most important force during cornering is the lateral force. It is possible to use a very simple expression for this force. With κ and F_z fixed, the typical relationship between α and F_y is illustrated in Figure 2.3. With small slip angles, the dependence is approximately linear. The slope of the curve in this linear region is defined as the lateral slip stiffness or cornering stiffness. It is denoted as $C_{F\alpha}$. Thus, the lateral force can be approximated with (Pacejka 2002):

$$F_y = C_{F\alpha}\alpha \tag{2.5}$$

Nonlinear Model A general model that accurately describes the lateral and longitudinal forces under combined slip conditions is complicated. A simplified model will be used. During pure lateral slip ($\kappa = 0$), the expres sion for the lateral force can be written as $F_y = F_y(\alpha, F_z)$. This can be described by the Magic Formula (Pacejka 2002, Bakker et al. 1989), which is shown in Figure 2.4. Note that the figure shows the normalized force, $\frac{F_y}{F_z}$, and that F_y does not vary linearly with F_z. The formula also describes the saturation properties of the tire forces. The parameters in the Magic Formula is explained in Table 2.1, especially note that several parameters depend on F_z. The expression for the formula is:

$$F_y = D\sin(C\arctan(B\alpha - E(B\alpha - \arctan(B\alpha)))) \tag{2.6}$$

Combined slip is described with $F_y = F_y(\alpha, \kappa, F_z)$, but it is more con venient in this work to express this as $F_y = F_y(\alpha, F_x, F_z)$. F_x is preferred

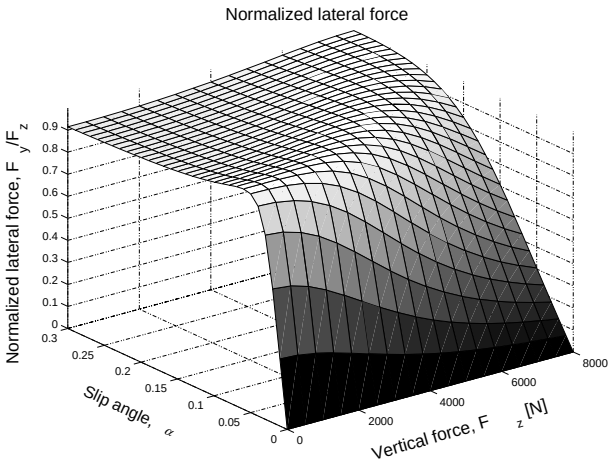

Figure 2.4 Normalized lateral force dependence on F_z and α.

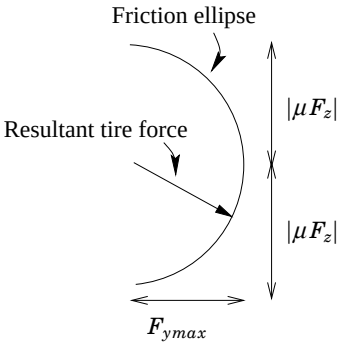

Figure 2.5 The friction ellipse for a tire. Note that F_{ymax} is given by the magic formula.

because it has a more direct physical meaning.

The simplest model for combined slip, i.e., combined braking and cor nering, is based on the friction ellipse. It is assumed that F_y and F_x cannot exceed their maximum values, F_{ymax} and F_{xmax}. The resultant tire force is assumed to be on the edge of the ellipse, $\left(\frac{F_y}{F_{ymax}(\alpha,F_z)}\right)^2 + \left(\frac{F_x}{F_{xmax}}\right)^2 = 1$,where $F_{ymax}(\alpha, F_z)$ is given by the Magic Formula and $F_{xmax} = \mu F_z$ (Wong 2001). The expression for the lateral force becomes:

$$F_y = F_{ymax}(\alpha, F_z)\sqrt{1 - \left(\frac{F_x}{\mu F_z}\right)^2} \qquad |F_x| \leq \mu F_z \tag{2.7}$$

The friction ellipse is illustrated in Figure 2.5. There is one ellipse for each tire, i.e., there will be four friction ellipses for a normal vehicle. F_x is the only force the controller can influence directly, F_y is affected by F_x through equation (2.7).

Table 2.1 Parameters in the Magic Formula.

Parameters	
$B = \frac{C_{F\alpha}}{CD}$	Stiffness factor
C	Shape factor
$D = \mu F_z$	Peak factor
E	Curvature factor
$C_{F\alpha} = c_1 \sin(2 \arctan(\frac{F_z}{c_2}))$	Cornering stiffness
c_1	Maximum cornering stiffness
c_2	Load at maximum cornering stiffness

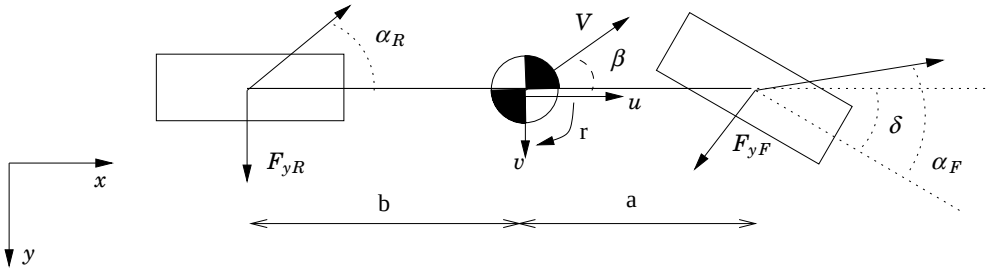

Figure 2.6 The bicycle model.

Chassis

Bicycle Model The bicycle model is a linear model that neglects the roll motion, assumes that the forward speed is constant, and approximates the four wheels with two wheels. These approximations make the model easy to understand and simple to use. The drawback is that it lacks roll, which is necessary for simulation and control design. The linear model will be used by the controller as a reference model.

The equations of motion for the two degree of freedom bicycle model (Pacejka 2002):

$$m(\dot{v} + ur) = F_{yF} + F_{yR} \tag{2.8}$$

$$I\dot{r} = aF_{yF} - bF_{yR} \tag{2.9}$$

The slip angles are expressed by:

$$\alpha_F = \delta - \frac{1}{u}(v + ar), \alpha_R = -\frac{1}{u}(v - br) \tag{2.10}$$

For small steering angles, the tire forces can be considered to be linear:

$$F_{yF} = C_F\alpha_F, F_{yR} = C_R\alpha_R \tag{2.11}$$

Combine the linear equations of motion with the linear tire forces equations, and the result is a linear vehicle model. This can be written in state space form, with parameters according to Table 2.2 and Figure 2.6:

Table 2.2 Bicycle model parameters.

Parameter	
V	Forward speed (constant)
C_F	Cornering stiffness, front wheels
C_R	Cornering stiffness, rear wheels
C	$C = C_F + C_R$
s	$s = \frac{C_F a + C_R b}{C}$
q^2	$q^2 = \frac{C_F a^2 + C_R b^2}{C}$
m	Vehicle mass
I	Vehicle moment of inertia about the z axis

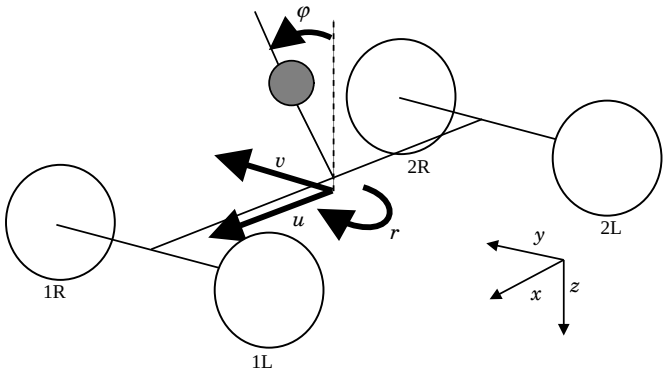

Figure 2.7 The states of the nonlinear model.

$$\begin{aligned} \dot{x} &= Ax + Bu \\ y &= Cx + Du \end{aligned} \tag{2.12}$$

$$\dot{x} = \begin{pmatrix} \dot{v} \\ \dot{r} \end{pmatrix}, u = \delta, y = \begin{pmatrix} v \\ r \end{pmatrix} \tag{2.13}$$

$$\begin{aligned} A &= -\begin{pmatrix} \frac{C}{mV} & V + \frac{Cs}{mV} \\ \frac{Cs}{IV} & \frac{Cq^2}{IV} \end{pmatrix}, \; B = \begin{pmatrix} \frac{C_F}{m} \\ \frac{C_F a}{I} \end{pmatrix} \\ C &= \begin{pmatrix} 1 & 0 \\ 0 & 1 \end{pmatrix}, \; D = \begin{pmatrix} 0 \\ 0 \end{pmatrix} \end{aligned} \tag{2.14}$$

Nonlinear Model The car body is modeled as a sprung mass according to Figure 2.7. The mass is considered to be connected to the wheel axles with torsional springs, i.e., the suspension is lumped together. The springs have the combined stiffness c_φ and combined damping k_φ. The stiffness c_φ is in reality nonlinear, since the springs only have a certain length. When

the springs get closer to their physical limits, the stiffness increases. This is especially important when the vehicle is close to rollover, because in this situation the springs on one side are severely compressed, and the roll angle cannot be assumed to be small. However, the model used here is only valid when all wheels have ground contact, and the stiffnesses are considered to be linear. The roll axis is considered to be fixed. The roll axis is tilted, and there is an angle, Θ_r, between the roll axis and the XY plane.

The model used has 4 degrees of freedom, and for this 5 states are needed. The motions considered are: u (longitudinal velocity), v (lateral velocity), r (yaw), and φ (roll). The front wheel axle is denoted as 1, and the rear wheel axle is denoted 2. The individual tires are denoted as com binations of the wheel axle and the side which the tire is situated, e.g., 1L corresponds to front axle, left side. The equations of motion are described in Equation 2.15 , and the parameters are shown in Figure 2.8, and explained in Table 2.3 (Pacejka 2002).

$$H(X)\dot{X} = F(X,U) \Rightarrow \dot{X} = H(X)^{-1}F(X,U) \tag{2.15}$$

Note the inverse of $H(X)$ in (2.15).

$$H(X) = \begin{pmatrix} m & 0 & -mh'\varphi & 0 & 0 \\ 0 & m & 0 & mh' & 0 \\ -mh'\varphi & 0 & I_z & (I_z\Theta_r - I_{xz}) & 0 \\ 0 & mh' & (I_z\Theta_r - I_{xz}) & (I_x + mh'^2) & (k_{\varphi 1} + k_{\varphi 2}) \\ 0 & 0 & 0 & 0 & 1 \end{pmatrix}$$

$$X = \begin{pmatrix} u \\ v \\ r \\ \dot{\varphi} \\ \varphi \end{pmatrix}, U = \begin{pmatrix} \delta \\ F_{xTot} \\ F_{yTot} \\ M_{Tot} \end{pmatrix}$$

$$F(X,U) = \begin{pmatrix} F_{xTot} + mrv + 2mh'\dot{\varphi}r \\ F_{yTot} - mru + mh'r^2\varphi \\ M_{Tot} - mh'vr\varphi \\ -mh'ur + (mh'^2 + I_y - I_z)r^2\varphi - (c_{\varphi 1} + c_{\varphi 2} - mgh')\varphi \\ \dot{\varphi} \end{pmatrix}$$

Vehicle Model

The nonlinear tire model (2.7) and the nonlinear chassis model (2.15) were combined and implemented in Simulink as S functions. This Simulink model was used for controller design and simulation. The combination is shown in Figure 2.10.

When the car rolls, load transfer will occur. As mentioned earlier, the roll axis is considered to be fixed. However, when wheel lift off occurs, the roll axis changes to be the point between the tires with ground contact and the ground. The equations of motion also change during wheel lift off. This

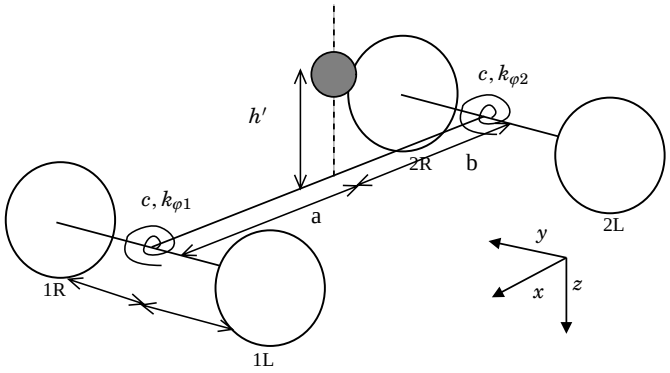

Figure 2.8 The parameters of the nonlinear model.

Table 2.3 Summary of the used terminology in the nonlinear model.

States (dynamic)	
u	Longitudinal velocity
v	Lateral velocity
r	Yaw rate
$\dot{\varphi}$	Roll rate
φ	Roll
Inputs (dynamic)	
δ	Steering angle
F_{xTot}	Total longitudinal force
F_{yTot}	Total lateral force
M_{Tot}	Total moment
Parameters (static)	
m	mass
h’	Distance from roll axis to CG
a	Distance from front to CG
b	Distance from rear to CG
Θ_r	Angle between roll axis and the XY plane
I_z	Moment of inertia about the z axis
I_y	Moment of inertia about the y axis
I_x	Moment of inertia about the x axis
I_{xz}	Product of inertia about the x z axes
$k_{\varphi i}$	Roll damping, axle i
$c_{\varphi i}$	Roll stiffness, axle i

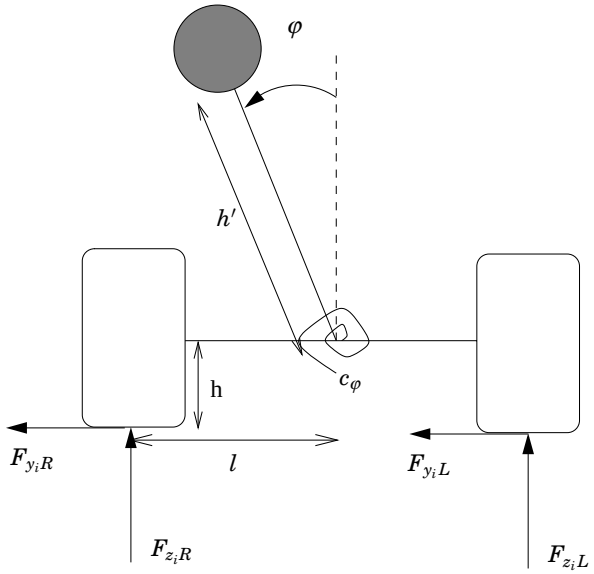

Figure 2.9 Moment balance for axle i.

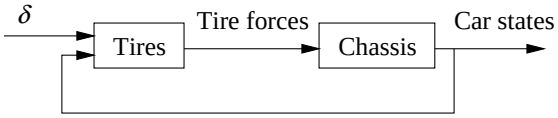

Figure 2.10 Combination of the tire model and chassis model.

is not modeled in the used model, i.e., wheel lift off is not included. The moment balance equation (see Figure 2.9) and force balance equations were used to calculate the tire forces corresponding to the two axles ($i = 1, 2$):

$$\begin{cases} F_{z_iR} + F_{z_iL} = F_{z_iTotal}, \begin{cases} F_{z_1Total} = \frac{mgb}{a+b} \\ F_{z_2Total} = \frac{mga}{a+b} \end{cases} \\ F_{y_iR} = F_{y_iRmax}(\alpha, F_{z_iR})\sqrt{1 - \left(\frac{F_{x_iR}}{\mu F_{z_iR}}\right)^2} \\ F_{y_iL} = F_{y_iLmax}(\alpha, F_{z_iL})\sqrt{1 - \left(\frac{F_{x_iL}}{\mu F_{z_iL}}\right)^2} \\ (F_{y_iR} + F_{y_iL})h + (F_{z_iR} - F_{z_iL})l - \dot{\varphi}k_{\varphi i} - \varphi c_{\varphi i} = 0 \end{cases} \tag{2.16}$$

This system of equations has to be solved numerically, which is done in every integration step in Simulink.

The forces coming from the four wheels are summed up to form the total forces and moment (see Figure 2.11). δ is assumed to be small, i.e., $\sin(\delta) = \delta$ and $\cos(\delta) = 1$.

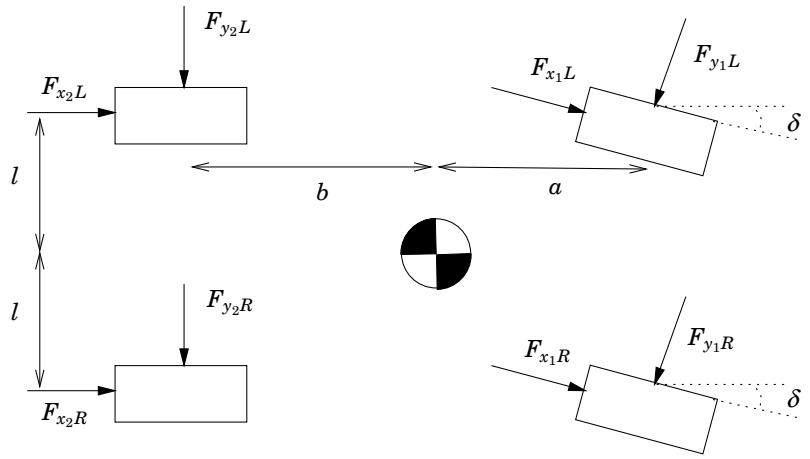

Figure 2.11 Tire forces.

$$
\begin{aligned}
F_{yTot} &= F_{y_1L} + F_{y_1R} + F_{y_2L} + F_{y_2R} + (F_{x_1L} + F_{x_1R})\delta \\
F_{xTot} &= F_{x_1L} + F_{x_1R} + F_{x_2L} + F_{x_2R} - (F_{y_1L} + F_{y_1R})\delta \\
M_{Tot} &= (F_{y_1L} + F_{y_1R})a - (F_{y_2L} + F_{y_2R})b + (F_{x_1L} + F_{x_1R})\delta a + \\
&\quad + (F_{x_1L} + F_{x_2L} + F_{y_1R}\delta - F_{x_1R} - F_{x_2R} - F_{y_1L}\delta)l
\end{aligned}
\tag{2.17}
$$

2.2 Vehicle Handling Characteristics

One of the controller's objectives is to make the vehicle follow a nominal trajectory, i.e., follow the driver's commands. Naturally, the mechanism behind rollover is also interesting. Thus, it is necessary to know how the vehicle reacts to the driver's commands, and some vehicle handling prop erties will be discussed.

Neutral steer, Understeer, and Oversteer

A vehicle can be neutral steer, understeer and oversteer. If the vehicle is neutral steer, then the same steering angle will give the same turning radius during different forward speeds. If the vehicle is understeer, then the same steering angle will give a bigger turning radius with increasing speed. Finally, if the vehicle is oversteer, then the same steering angle will give a smaller turning radius with increasing speed. Oversteer will also make the vehicle unstable when the forward speed passes a critical speed, V_{crit}. When $V > V_{crit}$, the required steering angle for any radius is zero, and the vehicle becomes unstable. This is why most vehicle are built to be understeer. The longitudinal placement of the CG is one of the parameters that most affect the vehicle steering type. If the CG is placed closer to the front wheels than to the rear wheels, the vehicle is understeer(Wong 2001). The car that is used in the simulations in this thesis is understeer.

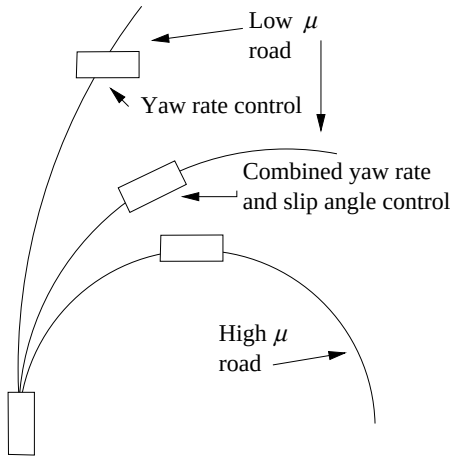

Figure 2.12 Yaw rate control compared to yaw rate and side slip angle control

Lateral Movement Control

An ordinary driver expects that the vehicle will have the same behavior regardless of the driving conditions. The trajectory desired by the driver is denoted as the nominal trajectory. A control system should try to follow the nominal trajectory, but there are physical limits. The adhesion between the tires and the road is one fundamental limit, which the lateral acceleration in steady state cannot exceed, $ma_y < \mu F_z = \mu mg$. This means that the yaw rate is limited, since $a_y = ur$ (steady state) $\Rightarrow r < \frac{\mu g}{u}$. In order to prevent a spin out, it is also necessary to limit the vehicle side slip angle, β, see equation (2.4). If only the yaw rate is controlled, the vehicle can still show some undesired properties. This is illustrated in Figure 2.12. One of the vehicles is driving on a road with high adhesion. This vehicle's trajectory defines the nominal trajectory. The other two vehicles have a controller and they are driving on a road with low adhesion. If the controller only controls the yaw rate, then the vehicle will deviate severely from the nominal trajectory, and it will start to skid. During skidding the tire forces are saturated, or close to saturation, and steering angle changes do not produce much moment. This is typical undesired behavior, because the driver can loose control of the car. However, if the controller controls both the yaw rate and the vehicle side slip angle a good compromise is achieved, and the car will not start to skid (van Zanten et al. 1996).

Rollover

The simplest way to reduce the risk of rollover, is to lower the center of gravity, or to make the vehicle wider. These solutions are efficient, but maybe not always applicable due to consumer demands. Another approach is to use slippery tires, which will make the available tire forces insufficient for inducing rollover. The latter suggestion will of course yield very poor handling characteristics, and it is not a realistic alternative (Forkenbrock et al. 2003).

The lateral acceleration is one of the most important sources of roll. The lateral acceleration is directly affected by the lateral force, F_y, and therefore is F_y important to control in order to control the roll. The total moment affects the yaw rate, which is coupled with the lateral acceleration.

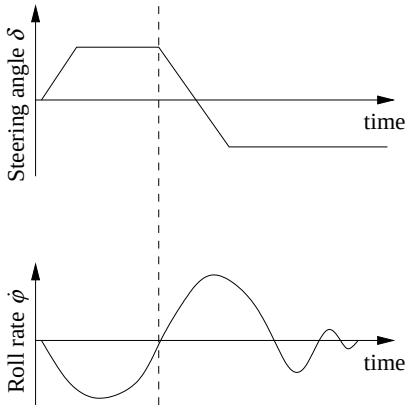

Figure 2.13 The Road Edge Recovery maneuver.

The total moment also affects the slip angle, which is the source of lateral forces. The longitudinal force F_x affects the velocity, which is the source of kinetic energy. With more kinetic energy the same maneuver, i.e. lateral displacement, will require more forces, and the maneuver will induce more roll. The different forces affects roll in the following order:

1. F_{yTot}
2. M_{Tot}
3. F_{xTot}

Test Maneuver

The best overall maneuver to evaluate dynamic rollover propensity is the Road Edge Recovery maneuver, according to Forkenbrock et al. (2003). The maneuver approximates the behavior of a startled driver that tries to get back to the correct lane position, after the driver accidently dropped two wheels off onto the shoulder. The maneuver starts with straight ahead driving, then the driver starts to increase the steering angle linearly, until the angle reaches some predefined value. The steering angle is held con stant until the magnitude of the roll rate is zero (this implies that at this moment, the roll angle is at a maximum point), and the steering angle is reversed (Forkenbrock et al. 2003). This will make the the maximum roll in the other direction even greater than the first one, especially if the steering frequency coincides with the natural frequency of the chassis. The maneu ver is illustrated in Figure 2.13. This maneuver will be used to evaluate the control design.

3. Rollover Detection

3.1 Measure

In order to prevent rollovers, it is necessary to know when a rollover is imminent. Thus, some kind of rollover measure is needed. The approach used is inspired by Dahlberg (2001), and is based on energy considerations.

The critical situation before rollover is when the potential energy reach es a local maximum, typically a saddle point. In this situation a small perturbation can make the car rollover. This is the basis of Dahlberg's measure. The measure is the lowest unstable local maximum point of the potential energy. However, before this unstable position is reached, the car will drive with only two wheels touching the ground, i.e., the other two wheels will be in the air. During the drive on two wheels, the car's han dling characteristics can be assumed to be completely different compared to driving with all wheels on the ground. The driver will probably loose control of the car (Gillespie 1992). Therefore, the critical situation will be when two tires lift off the ground. If wheel lift off can be prevented, then rollover is also prevented, since wheel lift off always occurs before rollover. In the following section it is assumed that the load transfer at the front axle is the same as the load transfer at the rear axle.

DEFINITION 3.1

Critical situation $\equiv$ two wheel lift off.

□

Just before wheel lift off, all the load has been transfered to one side, see Figure 3.1. In this situation, the lateral force is assumed to be the maximum possible force, given the vertical force, i.e., $F_y = \mu F_z$. When the car is approaching the critical situation, the potential energy is increasing. The total energy at the critical situation is denoted E_{crit}. If the sum of the potential energy (U) and the roll kinetic energy (T_{roll}), at any point, is above the critical total energy, then the critical position can be reached.

$$U + T_{roll} \equiv E_{roll} \geq E_{crit} \Rightarrow \text{Wheel lift off can occur}$$

$$\begin{cases} T_{roll} = \frac{1}{2}(I_{xx} + mh'^2)\dot{\varphi}^2 \\ U = \frac{1}{2}\varphi^2 c_\varphi - mgh'(1 - \cos(\varphi)) \end{cases} \Rightarrow$$

$$E_{roll} = \frac{1}{2}\varphi^2 c_\varphi - mgh'(1 - \cos(\varphi)) + \frac{1}{2}(I_{xx} + mh'^2)\dot{\varphi}^2 \tag{3.1}$$

First E_{crit} is calculated. The critical situation, or critical position, is shown in Figure 3.1. The moment equation about the roll axis:

$$F_z l - F_y h = (l - \mu h)mg \leq \varphi c_\varphi + \dot{\varphi} k_\varphi \tag{3.2}$$

The goal is to find the minimum E_{crit} that can induce wheel lift off. Two cases exist: the general transient case and the simpler steady state case.

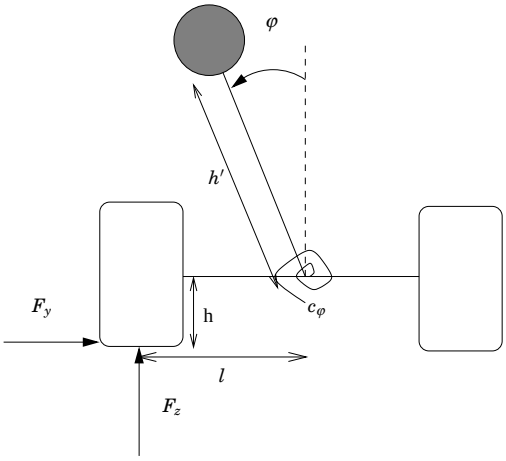

Figure 3.1 Critical situation.

- Transient case: The moment equation (3.2) is changed ($\leq$ is replaced by $=$) to $F_z l - F_y h = (l - \mu h)mg = \varphi c_\varphi + \dot{\varphi} k_\varphi$, in order to get the minimum E_{crit}. The critical energy is the minimum $E_{roll}(\varphi, \dot{\varphi})$ for which $F_z l - F_y h = \varphi c_\varphi + \dot{\varphi} k_\varphi$ is fulfilled.
- Steady state case: In the steady state case $\dot{\varphi} = 0$ and the moment balance (3.2) is changed ($\leq$ is replaced by $=$) to $F_z l - F_y h = (l - \mu h)mg = \varphi c_\varphi$, i.e., a position in equilibrium. This condition and (3.1) $\Rightarrow \varphi_{crit} \Rightarrow E_{crit}$.

To get nice values a normalized measure is defined:

DEFINITION 3.2

$$W_{WLO} \equiv \frac{E_{crit} - E_{roll}}{E_{crit}}$$

□

W_{WLO}, **W**arning: **W**heel **L**ift **O**ff .

If $W_{WLO} < 0$ then the car can reach the critical situation, i.e., wheel lift off. This measure do not take into account energy dissipation and driver input. However, it can give a warning when a wheel lift off can occur.

3.2 Results

Three scenarios were tested using the Road Edge Recovery maneuver:

- High CG (CG 0.4m above roll axis), high friction ($\mu = 1.0$)
- Low CG (CG 0.2m above roll axis), high friction ($\mu = 1.0$)
- High CG (CG 0.4m above roll axis), low friction ($\mu = 0.1$)

The parameters of the vehicle are given in section A.1. The Road Edge Recovery maneuver was performed in the following way:

- The steering angle was increased linearly with 5 rad/s.

Table 3.1 The calculated critical energies for the two vehicles.

	High CG	Low CG
Transient case [J]	526	548
Steady state case [J]	542	573

- When the steering angle reached 0.3 rad it was kept constant until the roll angle reached a maximum.
- The steering angle was now reversed linearly with 5 rad/s.
- When the steering angle reached 0.3 it was kept constant.

The calculated energies for the two different vehicle cases, high CG and low CG, are shown in Table 3.1. As can be seen, there is not much difference between the transient case and the steady state case. The transient case energy will be used in W_{WLO}. The transient case energy is chosen, because it is lower and therefore more conservative. Since the application is to provide safety, conservative is considered to be good.

In the following section, the three different test scenarios will be ex amined. For each scenario there is a plot. The plot visualizes the steering angle, W_{WLO} signal, and the four vertical tire forces. If the wheel lift off warning signal is below zero, then wheel lift off could happen. If one of the four vertical tire forces is below zero, then wheel lift off has occurred.

The first scenario is shown in Figure 3.2. The vertical lines in the figure mark the section were W_{WLO} is below zero, i.e., wheel lift off could be imminent. The arrows in the figure show were the vertical tire forces are below zero, and wheel lift off is a fact. The W_{WLO} measure seems to be working.

The second scenario is shown in Figure 3.3. In this scenario, the CG is situated lower than in the previous scenario, and the possibility for rollover or wheel lift off should be significantly reduced. There is no wheel lift off, and W_{WLO} is above zero at all times. The W_{WLO} measure seems to be working.

The third scenario is shown in Figure 3.4. In this case, the friction is low ($\mu = 0.1$), which means that the lateral forces are small, and it should not be possible to induce rollover or wheel lift off. There is no wheel lift off, and W_{WLO} is above zero at all times. The W_{WLO} measure seems to be working.

The different terms of the W_{WLO} during the Road Edge Recovery ma neuver, are visualized in Figure 3.5. The dominant term is the spring part of the potential energy. It can be seen that the kinetic energy is pumped into the potential energy during the second turn. Note that the potential energy does not have to be roll kinetic energy before it enters the mass spring system.

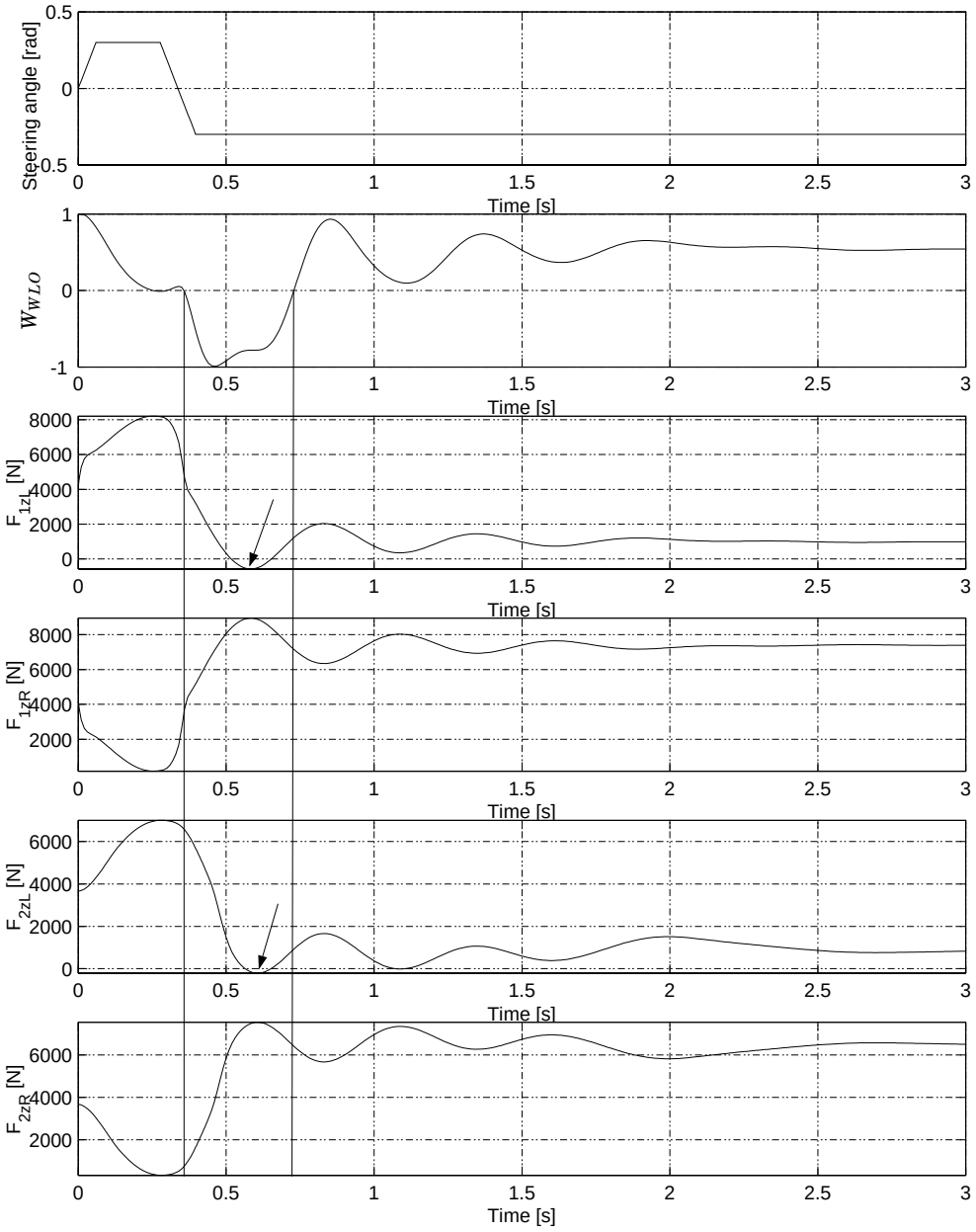

Figure 3.2 The first test scenario.

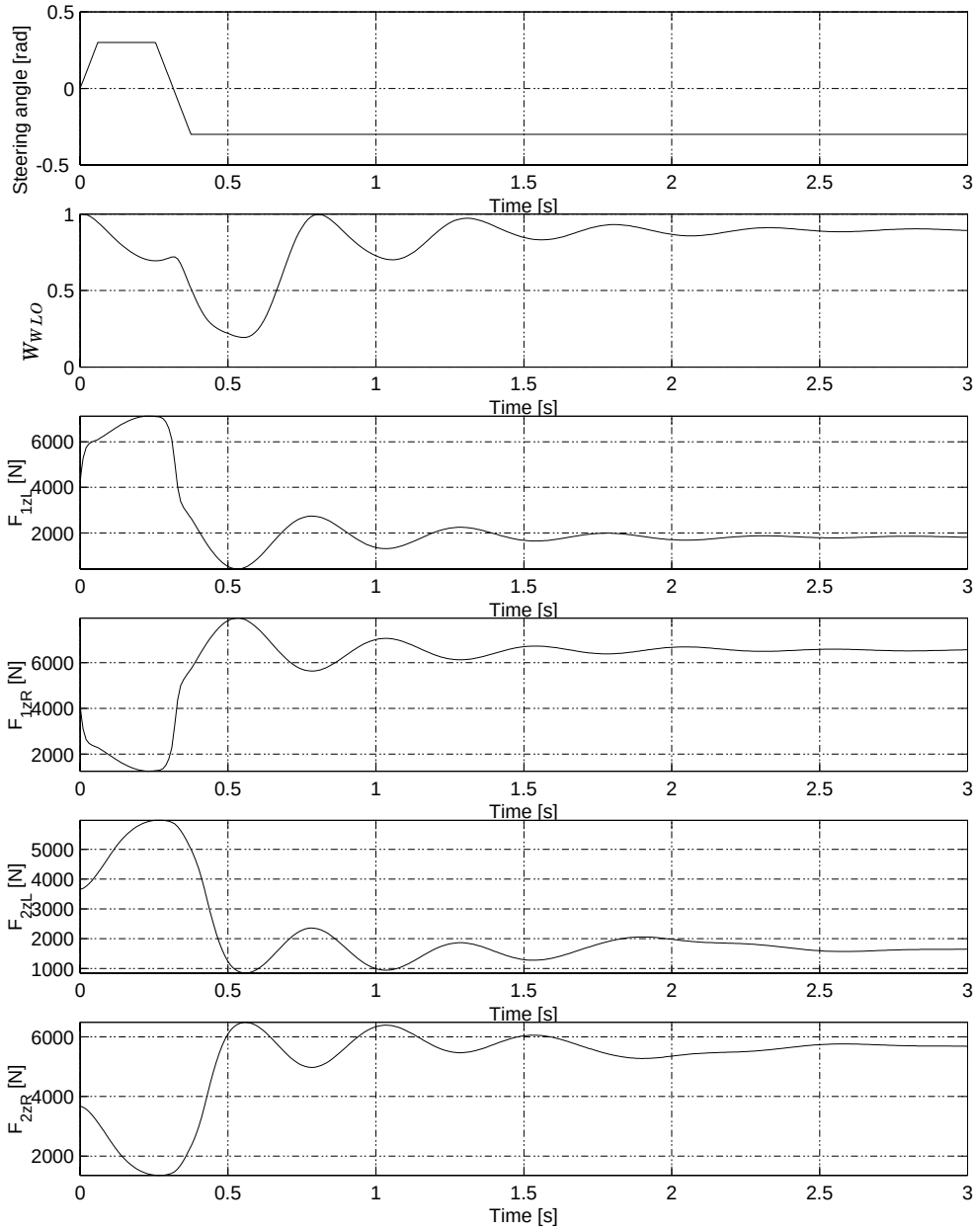

Figure 3.3 The second test scenario.

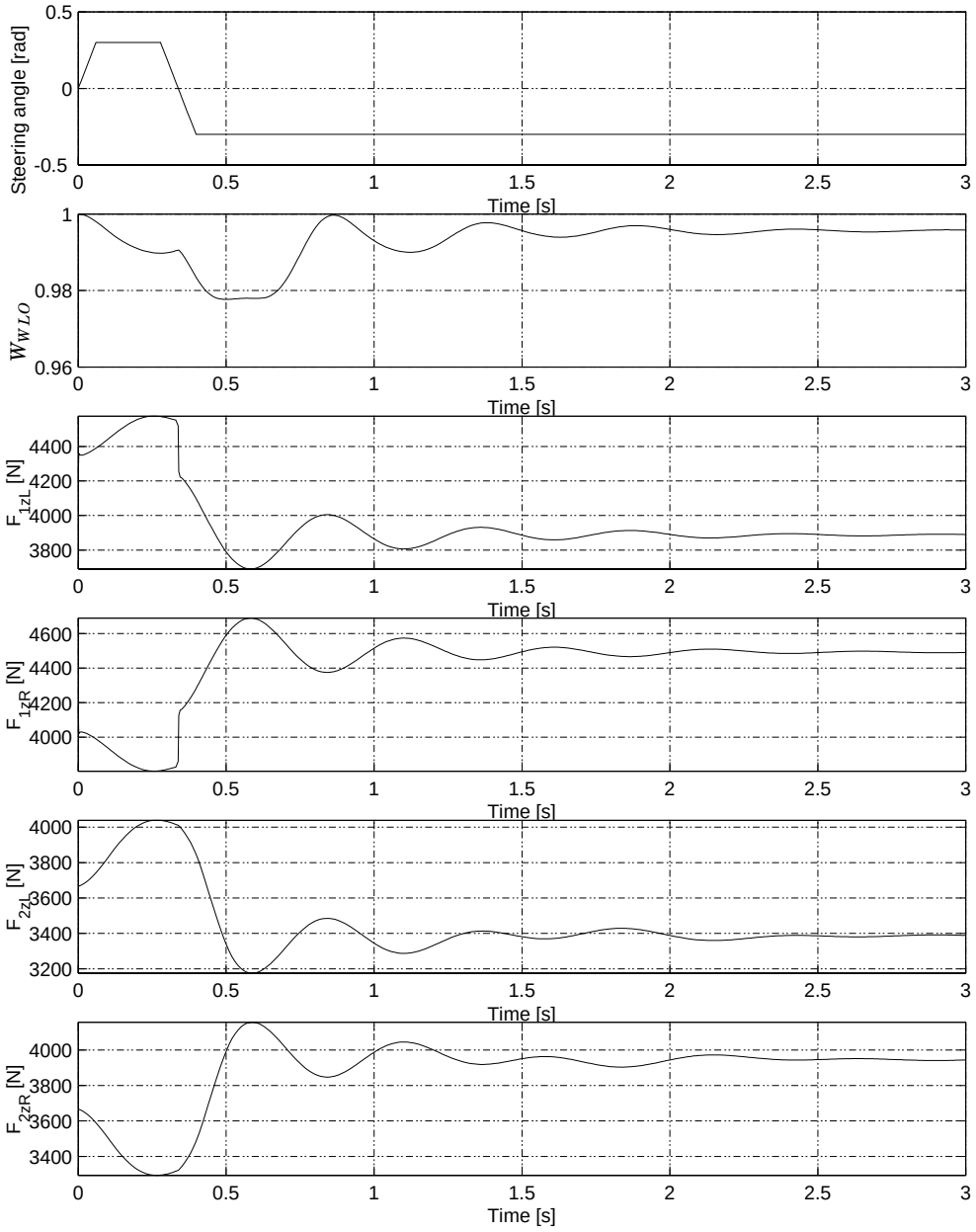

Figure 3.4 The third test scenario.

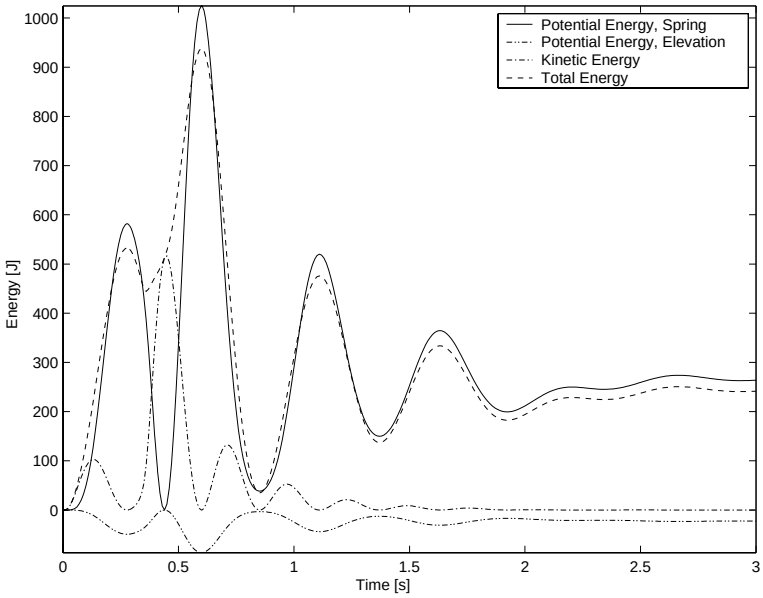

Figure 3.5 The terms in the total energy of the W_{WLO}.

4. Rollover Prevention

A gain scheduled discrete LQ (linear quadratic) controller following a lin ear reference model will be used. The LQ controller outputs the desired tire forces changes, ΔF_y, ΔF_x, and ΔM. These are then allocated to the four wheels by a control allocator. The total controller is shown in Figure 4.1.

The control problem has been divided into two subproblems, to design a controller, and to design a control allocator. The benefit is that the actuator constraints, i.e., tire force saturation, can be taken into account. The sep aration can essentially be done in the case where the same control action can be achieved with different actuator combinations (Härkegård 2003).

The controller is supposed to be implemented in a computer, therefore, discrete theory will be used. The sampling rate was chosen to be fast, $f = 100Hz$, in order to minimize the influence that the sampling rate has on the performance of the system. Furthermore, the estimation problem is not considered, and noise is neglected.

4.1 LQ Controller

The LQ (linear quadratic) controller is a state feedback controller, i.e., $U(k) = -L(k)X(k)$, that minimizes a cost function, J. The cost function consists of linear quadratic terms of the states and of the control signal, hence the name linear quadratic. The structure of the cost function is essen tially $J = \int |U(t)|^2 + |X(t)|^2 dt$. The more formal and general discrete time cost function is:

$$\begin{aligned} J = E \ \sum_{k=0}^{N-1} (X^T(kh)Q_1X(kh) + 2X^T(kh)Q_{12}U(kh) \\ + U^T(kh)Q_2U(kh)) + X^T(Nh)Q_0X(Nh) \end{aligned} \tag{4.1}$$

The Q matrices in (4.1) are called weighting matrices or penalty matri ces. The penalty matrices make it possible to put different penalty on the control signal and the states. The penalties are selected in manner that gives the close system the desired behavior. The penalties must also be set in a way that the controller signal is feasible and achievable. This is an iterative process, the penalties are changed, and simulations are done to see what effect the changes had. If the changes did not give the desired properties, then adjust them again and so forth. The used penalty matrices for the controller design are given in section A.2.

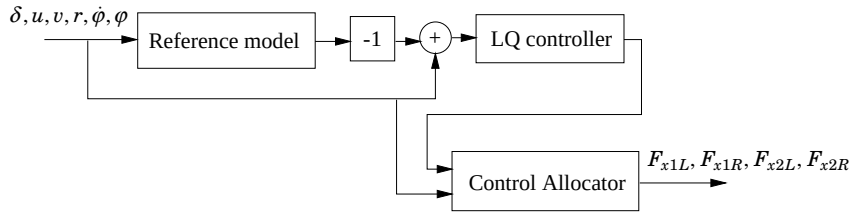

Figure 4.1 The total controller.

The use of a quadratic loss function can be justified by the quadratic wheel lift off warning measure, W_{WLO}. The W_{WLO} measure should be as low as possible. However, if the roll angle rate is penalized, then it is more expensive to minimize the roll angle. A small penalty on the roll angle rate avoids this.

One good property of the LQ controller is that it gives a stable closed loop system. However, this is only true for feedback loop with a linear system, and while the control signal does not saturate. With the nonlinear vehicle model and possible saturation in the tires, stability is not guaran teed.

In the general case $L(k)$ is time varying. For simplicity the stationary controller will be used. The stationary controller is obtained by solving the algebraic Riccati equation. A more in depth discussion on LQ controllers is provided by Åström & Wittenmark (1997).

4.2 Gain Scheduling

Gain scheduling is based on knowledge about how the process dynamics changes under different operating conditions. The operating condition is measured, and the controller parameters are changed with the operating conditions. The plant is linearized in several operating points, and a con troller is designed for each point. The total controller output is then a weighted sum of the different controllers. The controller corresponding to the linearization point closest to the actual states will have the biggest con tribution to the control signal. A thorough presentation of gain scheduling is given in Åström & Wittenmark (1995).

Using linearization in different points is useful in the vehicle case, be cause the system dynamics radically changes with the yaw rate, r. Lateral acceleration is the primary cause of roll, and $a_y = \dot{v} + ur$. A linearization yields: $a_y \approx a_{y0} + \dot{v} + u_0\Delta r + r_0\Delta u$. The coefficient, r_0, will have different signs depending on if the vehicle is turning left or turning right. If the system is linearized in straight ahead driving, $r = 0$, then a_y will only depend on r. The yaw rate is therefore one of the variables which is crucial for the operating point. The vehicle forward speed, u, is the main source of kinetic energy, and higher speed will give bigger lateral forces during a specific maneuver. The forward speed is therefore also crucial for the operating point.

For each linearization point there is a state feedback vector, L, and a weighting function, θ. The weighting function assumes the value one when the operating conditions coincides with the corresponding lineariza tion point. The sum of all weighting functions is always one. Nine lineariza tion points were chosen in the ur plane, according to Figure 4.2. The total state feedback law becomes:

$$U = \sum_{i=1}^{9} -\theta_i(X)L_i\Delta X \tag{4.2}$$

The stationary points were found using the Matlab command *trim*, the points are shown in section A.3. The system was linearized at the sta tionary points with the Matlab command *linmod*. For each point a state

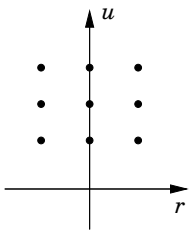

Figure 4.2 The linearization points.

feedback vector was created with the Matlab command *dlqr*, using the penalty matrices in A.2. See *Matlab on line documentation* (n.d.) for more details regarding the used commands.

4.3 Reference Values and Controller Activation

The linear bicycle model (2.14) is used as a reference model, and it provides the reference values for the lateral velocity and the yaw rate, v_{ref} and r_{ref}. r_{ref} is limited in order to not exceed the available amount of friction (see section 2.2). The limited yaw rate is denoted r'_{ref}, and it is defined as follows:

$$r'_{ref} = \begin{cases} \frac{\mu g}{u}, \; r_{ref} > \frac{\mu g}{u} \\ r_{ref}, \; r_{ref} \leq \frac{\mu g}{u} \end{cases}$$

This will make the controller try to maintain this linear behavior during all operating conditions.

The controller is only activated when W_{WLO}, is below a threshold. The threshold has to be found by simulation and testing. The W_{WLO} threshold was chosen to be 0.3. Thus, the controller is activated if $WLOW < 0.3$.

The reference values for v and r are taken from the linear reference model. The reference values for u, $\dot{\varphi}$, and φ are set to be zero. The forward velocity should go to zero in a dangerous situation ($WLOW <$ threshold), this will prevent to large forces to be induced. The roll and roll rate should also go to zero in a dangerous situation ($WLOW <$ threshold), this will prevent the roll to become to large, i.e., prevent wheel lift off.

The controller should be turned on and off in a smooth way, therefore a weighting function ψ is introduced. ψ is zero when W_{WLO} is above 0.3, and increases quadratically to one, when W_{WLO} is between 0.3 and zero.

$$\psi = \begin{cases} 0, \; WLOW > 0.3 \\ \frac{(0.3 - WLOW)^2}{0.3^2}, \; 0 \leq WLOW \leq 0.3 \\ 1, \; WLOW < 0 \end{cases}$$

All the reference values are multiplied with ψ, to make the on off transition continuous.

$$\Delta u = \psi(u_{actual} - 0)$$

$$\Delta v = \psi(v_{actual} - v_{ref})$$

$$\Delta r = \psi(r_{actual} - r'_{ref})$$

$$\Delta\dot{\varphi} = \psi(\dot{\varphi}_{actual} - 0)$$
$$\Delta\varphi = \psi(\varphi_{actual} - 0)$$
$$\Delta X = (\Delta u\ \Delta v\ \Delta r\ \Delta\dot{\varphi}\ \Delta\varphi)^T$$

4.4 Control Allocation

The benefit of using a separate control allocator is that actuator saturation can be taken into account to some extent. The control actuator's purpose is to solve an under determined system of equations under constraints. The control allocator is given the desired total control action, *virtual control input*, in this thesis denoted $U(t) \in \mathbb{R}^k$. The control allocator outputs the *true control output*, in this thesis denoted $T(t) \in \mathbb{R}^m$, $m > k$. The general relationship between those two quantities is, $g(T(t)) = U(t)$. But in the literature, almost only the linear case is studied, $GT(t) = U(t)$, where G is a $k \times m$ matrix with rank k. For the linear case there exists many algorithms. Solving the nonlinear problem is done with constrained non linear programming, but this can be time consuming and it is probably not suitable for real time applications (Härkegård 2003).

The brakes are chosen as actuators, because they are cheaper than other actuators, and they are often already in the car. However, there are other actuators that provides more freedom and less possibility of saturation of the control action, e.g., active steering (Ackermann et al. 1999). If only the brakes are used as actuators then the following constraints apply:

$$\mu F_{zi} < F_{xi} < 0,\ i = \text{ 1L, 1R, 2L, 2R} \tag{4.3}$$

If it is also can be assumed that it is possible to apply a driving torque to the wheels, i.e., a forward force, then the constraints will be:

$$|F_{xi}| \leq \mu F_{zi},\ i = \text{ 1L, 1R, 2L, 2R} \tag{4.4}$$

In this work it is assumed that the actuators can give both forward and backward forces (4.4). Note that the actuator constraints depends on the lateral load transfer, i.e., F_z. Therefore, will the size of the available half ellipses be non uniform. An example of the available forces configuration is shown in Figure 4.3.

The control allocation problem is to find $T(t) = (F_{x1L}\ F_{x1R}\ F_{x2L}\ F_{x2R})^T$ that will give the desired control action $U(t)$. The relationship between T and U is (given by equations (2.7) and (2.17)):

$$U = g(X, T) = A \begin{pmatrix} h(X,T) \\ T \end{pmatrix}$$
$$U = (F_{yTot}\ F_{xTot}\ M_{Tot})^T$$

$$A = \begin{pmatrix} 1 & 1 & 1 & 1 & \delta & \delta & 0 & 0 \\ -\delta & -\delta & 0 & 0 & 1 & 1 & 1 & 1 \\ (a-\delta l) & (a+\delta l) & -b & -b & (\delta a + l) & (\delta a - l) & l & -l \end{pmatrix}$$

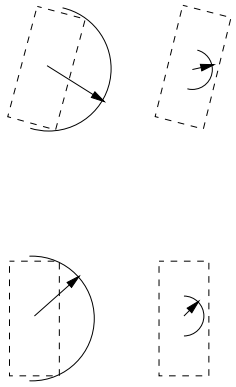

Figure 4.3 An example of a configuration of available forces for each tire, under the condition, $|F_x| \leq \mu F_z$, and lateral load transfer.

$$T(t) = (F_{x1L}\ F_{x1R}\ F_{x2L}\ F_{x2R})^T$$

$$h(X,T) = \begin{pmatrix} F_{ymax}(\alpha_1, F_{z1L})\sqrt{1 - \left(\frac{F_{x1L}}{\mu F_{z1L}}\right)^2} \\ F_{ymax}(\alpha_1, F_{z1R})\sqrt{1 - \left(\frac{F_{x1R}}{\mu F_{z1R}}\right)^2} \\ F_{ymax}(\alpha_2, F_{z2L})\sqrt{1 - \left(\frac{F_{x2L}}{\mu F_{z2L}}\right)^2} \\ F_{ymax}(\alpha_2, F_{z2R})\sqrt{1 - \left(\frac{F_{x2R}}{\mu F_{z2R}}\right)^2} \end{pmatrix}$$

This can also be expressed as:

$$x = (F_{y1L}\ F_{y1R}\ F_{y2L}\ F_{y2R}\ F_{x1L}\ F_{x1R}\ F_{x2L}\ F_{x2R})^T$$

$$F_{yi} = F_{ymax}(\alpha_i, F_{zi})\sqrt{1 - \left(\frac{F_{xi}}{\mu F_{zi}}\right)^2},\ i = \text{1L, 1R, 2L, 2R} \tag{4.5}$$

$$U = (F_{yTot}\ F_{xTot}\ M_{Tot})^T$$

$$A = \begin{pmatrix} 1 & 1 & 1 & 1 & \delta & \delta & 0 & 0 \\ -\delta & -\delta & 0 & 0 & 1 & 1 & 1 & 1 \\ (a-\delta l) & (a+\delta l) & -b & -b & (\delta a + l) & (\delta a - l) & l & -l \end{pmatrix}$$

$$Ax = U \tag{4.6}$$

The control allocator should solve the equation (4.6) in the best possible way under the constraints (4.4). Thus, the forces $(F_{x1L}\, F_{x1R}\, F_{x2L}\, F_{x2R}) = T$ have to be found. How to define the best possible way is non trivial, but a simple candidate is, $x^* = \arg\min_x ||Ax - U||_2$. $\arg\min_x f(x)$ gives the x that minimizes $f(x)$, and $||\cdot||_2$ is the standard two norm, i.e., $||x||_2 = \sqrt{\sum_i x_i^2}$.

Three different approaches were tested:

- Nonconvex Nonlinear Optimization
- Linear Approximation

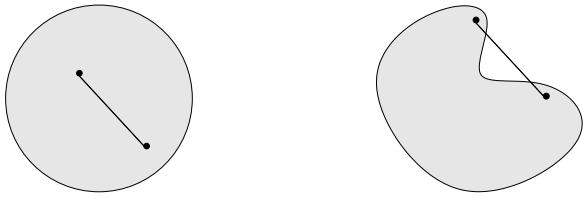

Figure 4.4 *Left* Convex set. *Right* Nonconvex set.

- Convex Optimization

The approaches will be explained in detail, but first some basics in opti mization theory.

Optimization

This section follows Boyd & Vandenberghe (2004), where also more details can be found regarding convex optimization. A general formulation of an optimization problem is:

$$\begin{aligned} &\underset{x}{\text{minimize}}\ f_0(x) \\ &\text{subject to}\ f_i(x) \leq b_i,\ i = 1, ..., m \end{aligned}$$

The general optimization problem is hard, but if the functions, f_i, $i = 0, ..., m$, are convex, efficient methods exist. A set is convex if the line, between two points in the set, is in the set, see Figure 4.4. A function, f, is convex if f is defined for a convex set, and $f(\theta x + (1-\theta)y) \leq \theta f(x) + (1-\theta)f(y)$, $0 \leq \theta \leq 1$.

Two specific optimization problems will be especially useful, the least squares problem and the second order cone program.

Least Squares Problem The least squares problem:

$$\underset{x}{\text{minimize}}\ ||Ax - b||_2^2 \quad (\Leftrightarrow \underset{x}{\text{minimize}}\ ||Ax - b||_2) \tag{4.7}$$

The weighted least squares problem has an analytical solution, which ma kes it fast to solve. The general solution is given by the pseudo inverse, $A^\dagger$. Let $A \in \mathbb{R}^{m \times n}$, with $\text{rank}(A) = r$, have the singular value decomposition

$$A = U \begin{matrix} \Sigma_r & 0 \\ 0 & 0 \end{matrix} V^T$$

then the pseudo inverse is defined as

$$A^\dagger = V^T \begin{matrix} \Sigma_r^{-1} & 0 \\ 0 & 0 \end{matrix} U$$

Then the problem

$$\begin{aligned} &\underset{x \in \Omega}{\text{minimize}}\ ||x||_2 \\ &\Omega = \arg\min_x ||Ax - b||_2 \end{aligned}$$

where arg min gives the set of minimizing solutions, has the solution $x = A^{\dagger}b$. This solution can be modified to be used with a weighted 2 norm, $||x||_W = ||Wx||_2$, where W is assumed to be non singular. The new problem

$$\begin{aligned} &\underset{x\in\Omega}{\text{minimize}} \ ||Wx||_2 \\ &\Omega = \arg\min_x ||Ax-b||_2 \end{aligned}$$

can be solved with the transformation $Wx = e \Leftrightarrow x = W^{-1}e$. The solution is $x = W^{-1}e = W^{-1}(AW^{-1})^{\dagger}b$ (Boyd & Vandenberghe 2004).

Second Order Cone Program Another type of problem, that will be useful, is the second order cone program, SOCP:

$$\begin{aligned} &\text{minimize } f^T x \\ &\text{subject to } \begin{cases} ||A_i x + b_i||_2 \leq c_i^T x + d_i, \ i = 1, ..., m \\ Fx = g \end{cases} \end{aligned} \tag{4.8}$$

This type of problem can be solved efficiently with interior point methods (Boyd & Vandenberghe 2004).

The three approaches will be presented first, then the results of these approaches will be given.

Nonconvex Nonlinear Optimization

The allocation problem is nonconvex, and nonconvex problems are hard to solve (Boyd & Vandenberghe 2004). The advantage with trying to solve the original problem, is that no transformation of the problem is necessary. The major disadvantage is that no efficient algorithm is available.

The command *fgoalattain*, from the optimization toolbox in Matlab, was used to solve the nonlinear problem. The command makes it possible to solve a weighted multidimensional nonlinear constrained optimization problem, see *Matlab on line documentation* (n.d.) for more details.

Linear Approximation

The most straightforward way to make the problem easier, is to linearize around the last used point, i.e., F_{x1L0}, F_{x1R0}, F_{x2L0}, F_{x2R0}. The linearized version of the problem is illustrated in Figure 4.5. The linearized version can then be solved using pseudo inverse methods mentioned before. The constraints are neglected, but an effort to compensate for them is made with the weights in the norm used. The weights are chosen to be the inverse of the corresponding available amount of force (Härkegård 2003):

$$W = \begin{pmatrix} \frac{1}{\mu F_{z1L0}} & 0 & 0 & 0 \\ 0 & \frac{1}{\mu F_{z1R0}} & 0 & 0 \\ 0 & 0 & \frac{1}{\mu F_{z2L0}} & 0 \\ 0 & 0 & 0 & \frac{1}{\mu F_{z2R0}} \end{pmatrix}$$

Forces that are less constrained (μF_z large) are less penalized than forces which are more constrained (μF_z small). This will take the constraints into

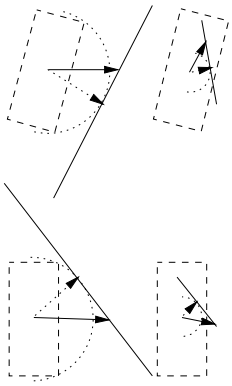

Figure 4.5 Available forces with the linear approximation. The dotted ellipses is the original available forces. The dotted arrows are the last used point.

account to some extent, but nothing is guaranteed. If the calculated forces violates the constraints, they are simply cut at the boundary.

If the changes are small, then the approximation is very good. However, the approximation can also be extremely bad. When F_x is close to zero, then a change in F_x will give a small change in F_y, which is a bad approximation if the change in F_x is large. When F_x is close to its maximum, μF_z, then a small change in F_x will give a large change in F_y. This is a bad approximation if the change in F_x is large.

The linearization:

$$U = g(X,T) = A_1 T + A_2 h(X,T)$$

With $T = (F_{x1L}\ F_{x1R}\ F_{x2L}\ F_{x2R})^T$ and $X = (u\ v\ r\ \dot{\varphi}\ \varphi)^T$, and A_1, A_2, and $h(X,T)$ are given by

$$A_1 = \begin{pmatrix} 1 & 1 & 1 & 1 \\ -\delta & -\delta & 0 & 0 \\ (a-\delta l) & (a+\delta l) & -b & -b \end{pmatrix}$$

$$A_2 = \begin{pmatrix} \delta & \delta & 0 & 0 \\ 1 & 1 & 1 & 1 \\ (\delta a + l) & (\delta a - l) & l & -l \end{pmatrix}$$

$$h(X,T) = \begin{pmatrix} F_{ymax}(\alpha_1, F_{z1L})\sqrt{1 - \left(\frac{F_{x1L}}{\mu F_{z1L}}\right)^2} \\ F_{ymax}(\alpha_1, F_{z1R})\sqrt{1 - \left(\frac{F_{x1R}}{\mu F_{z1R}}\right)^2} \\ F_{ymax}(\alpha_2, F_{z2L})\sqrt{1 - \left(\frac{F_{x2L}}{\mu F_{z2L}}\right)^2} \\ F_{ymax}(\alpha_2, F_{z2R})\sqrt{1 - \left(\frac{F_{x2R}}{\mu F_{z2R}}\right)^2} \end{pmatrix}$$

Truncated Taylor expansion gives

$$h(X,T) \approx h_o(X,T_0) + \frac{\partial h(X,T_0)}{\partial T}(T - T_0)$$

$$\Rightarrow A_2 h(X,T) \approx A_2(h_0(X,T_0) + \frac{\partial h(X,T_0)}{\partial T}(T - T_0))$$

$$\Rightarrow U \approx A_1 T + A_2(h_0(X,T_0) + \frac{\partial h(X,T_0)}{\partial T}(T - T_0))$$

$$\Leftrightarrow U + A_2(\frac{\partial h(X,T_0)}{\partial T}T_0 - h_0(X,T_0)) \approx (A_1 + A_2\frac{\partial h(X,T_0)}{\partial T})T$$

Which is linear in T, and can be written on the form

$$U' = A'_{lin}T$$

h_0 and $\frac{\partial h(X,T_0)}{\partial T}$ are given by

$$h_0(X,T) = \begin{pmatrix} F_{ymax}(\alpha_1, F_{z1L})\sqrt{1 - \left(\frac{F_{x1L0}}{\mu F_{z1L}}\right)^2} \\ F_{ymax}(\alpha_1, F_{z1R})\sqrt{1 - \left(\frac{F_{x1R0}}{\mu F_{z1R}}\right)^2} \\ F_{ymax}(\alpha_2, F_{z2L})\sqrt{1 - \left(\frac{F_{x2L0}}{\mu F_{z2L}}\right)^2} \\ F_{ymax}(\alpha_2, F_{z2R})\sqrt{1 - \left(\frac{F_{x2R0}}{\mu F_{z2R}}\right)^2} \end{pmatrix}$$

$$\frac{\partial h(X,T_0)}{\partial T} = \begin{pmatrix} \frac{-F_{x1L0}F_{ymax}(\alpha_1,F_{z1L})}{(\mu F_{z1L})^2\sqrt{1-\left(\frac{F_{x1L0}}{\mu F_{z1L}}\right)^2}} \\ \frac{-F_{x1R0}F_{ymax}(\alpha_1,F_{z1R})}{(\mu F_{z1R})^2\sqrt{1-\left(\frac{F_{x1R0}}{\mu F_{z1R}}\right)^2}} \\ \frac{-F_{x2L0}F_{ymax}(\alpha_2,F_{z2L})}{(\mu F_{z2L})^2\sqrt{1-\left(\frac{F_{x2L0}}{\mu F_{z2L}}\right)^2}} \\ \frac{-F_{x2R0}F_{ymax}(\alpha_2,F_{z2R})}{(\mu F_{z2R})^2\sqrt{1-\left(\frac{F_{x2R0}}{\mu F_{z2R}}\right)^2}} \end{pmatrix}$$

The problem to be solved is

$$\begin{aligned} &\underset{x\in\Omega}{\text{minimize}} \; ||WT||_2 \\ &\Omega = \arg\min_T ||A'_{lin}T - U'||_2 \end{aligned}$$

The solution is $T = W^{-1}(A'_{lin}W^{-1})^{\dagger}U'$.

Convex Optimization

If the equalities (4.5) are relaxed to be inequalities instead (4.9), then the new set will be convex, see Figure 4.6.

$$\left(\frac{F_{yi}}{F_{ymax}(\alpha_i, F_{zi})}\right)^2 + \left(\frac{F_{xi}}{\mu F_{zi}}\right)^2 \leq 1 \qquad (4.9)$$

$$i = \text{ 1L, 1R, 2L, 2R}$$

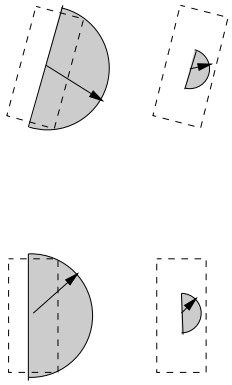

Figure 4.6 Available forces with the convex approximation.

$$F_{yi}F_{ymax}(\alpha_i, F_{zi}) \geq 0$$

The last inequality demands that F_{yi} will have the same sign as F_{ymax}. Without this condition, (4.9) gives an ellipse, not the desired half ellipse.

The new relaxed problem can be posed as a second order cone program, SOCP. There exist methods for solving these types of problems too, as mentioned earlier.

The optimization variables are:

$x = (F_{y1L}\ F_{y1R}\ F_{y2L}\ F_{y2R}\ F_{x1L}\ F_{x1R}\ F_{x2L}\ F_{x2R})^T$ and γ, where γ is a slack variable. The inequalities (4.9), can easily be written on the form $||A_i x|| < 1$, e.g.,

$$\left(\frac{F_{y1L}}{F_{ymax}(\alpha_1, F_{z1L})}\right)^2 + \left(\frac{F_{x1L}}{\mu F_{z1L}}\right)^2 \leq 1$$

$$\Updownarrow$$

$$||A_{1L}x||_2 = \left\| \begin{pmatrix} \frac{1}{F_{ymax1L}} & 0 & 0 & 0 & 0 & 0 & 0 & 0 \\ 0 & 0 & 0 & 0 & 0 & 0 & 0 & 0 \\ 0 & 0 & 0 & 0 & 0 & 0 & 0 & 0 \\ 0 & 0 & 0 & 0 & 0 & 0 & 0 & 0 \\ 0 & 0 & 0 & 0 & \frac{1}{\mu F_{z1L}} & 0 & 0 & 0 \\ 0 & 0 & 0 & 0 & 0 & 0 & 0 & 0 \\ 0 & 0 & 0 & 0 & 0 & 0 & 0 & 0 \\ 0 & 0 & 0 & 0 & 0 & 0 & 0 & 0 \end{pmatrix} \begin{pmatrix} F_{y1L} \\ F_{y1R} \\ F_{y2L} \\ F_{y2R} \\ F_{x1L} \\ F_{x1R} \\ F_{x2L} \\ F_{x2R} \end{pmatrix} \right\|_2 \leq 1$$

and so forth.

In order to try to force the solution to be on the boundary of the ellipse, i.e., the unrelaxed constraints (4.5) should be fulfilled, it is necessary to include this condition in the expression that will be minimized. If the lat eral forces are chosen to be as close to the maximal lateral force available as possible, then the solution will be on the ellipse. One way to formalize

this in pseudo code is:

$$
\begin{aligned}
&\text{While equation (4.5) not fulfilled} \\
&\{ \\
&\quad \text{minimize} \sum_{i=1L,1R,2L,2R} (|F_{ymaxi}| - |F_{yi}|) + \zeta\gamma \\
&\quad \text{subject to} \begin{cases} F_{yi}F_{zi} \geq 0,\ i = 1L, 1R, 2L, 2R \\ ||Ax - U||_2 < \gamma \\ ||A_i x||_2 < 1,\ i = 1L, 1R, 2L, 2R \end{cases} \\
&\quad \zeta := \tfrac{\zeta}{2} \\
&\}
\end{aligned}
\tag{4.10}
$$

After the optimization is completed, the constraint condition (4.5) is tested. If it is not valid, then the weight ζ is lowered to half of the original value, $\zeta := \frac{\zeta}{2}$, and the optimization is redone. This time, the objective to minimize $||Ax - U||_2$, has lower priority, and the new solution is hopefully on the ellipse. If the new solution does not fulfill equation (4.5), repeat the procedure again. In this way a solution fulfilling the original constraints will be found.

The optimizations were done with SeDuMi using the parser YALMIP.

4.5 Results

Control Allocation

Without a working control allocator, the total control system cannot be tested. Therefore, the results of the testing of the three different control allocation approaches are presented first. The test maneuver is the Road Edge Recovery maneuver, which was used in the detection part as well.

Initial test showed that the demand that all three, F_{yTot}, F_{xTot}, M_{Tot} quantities should be adjustable by the control allocator, degraded the al locators performance. Often the result was a bad compromise. Since F_{yTot} and M_{Tot} are the two most important quantities to control for good perfor mance (see section 2.2), F_{xTot} was removed from U.

$$U = (F_{yTot}\, M_{Tot})^T$$

The system is still controllable, and the performance increases, since no bad compromises have to be made.

The three different solutions need different amounts of execution time to accomplish their task. Mean values of the different execution times are presented in Table 4.1. The linear approximation is clearly the fastest one, and there is not much difference between the nonlinear nonconvex and the convex approach. However, the execution time of the nonlinear nonconvex approach varied greatly, which is not desired in a real time application. Both of them are too slow, but this is run in Matlab. With proper tweaking and implementation of the code, it could be considerably faster.

Table 4.1 Mean execution times.

	Nonlinear	Linear	Convex
Mean execution time [s]	1.80	0.0044	1.42

Nonlinear nonconvex Approach

The desired tire forces compared with the actual tire forces are shown in Figure 4.7. The control signals are shown in Figure 4.8.

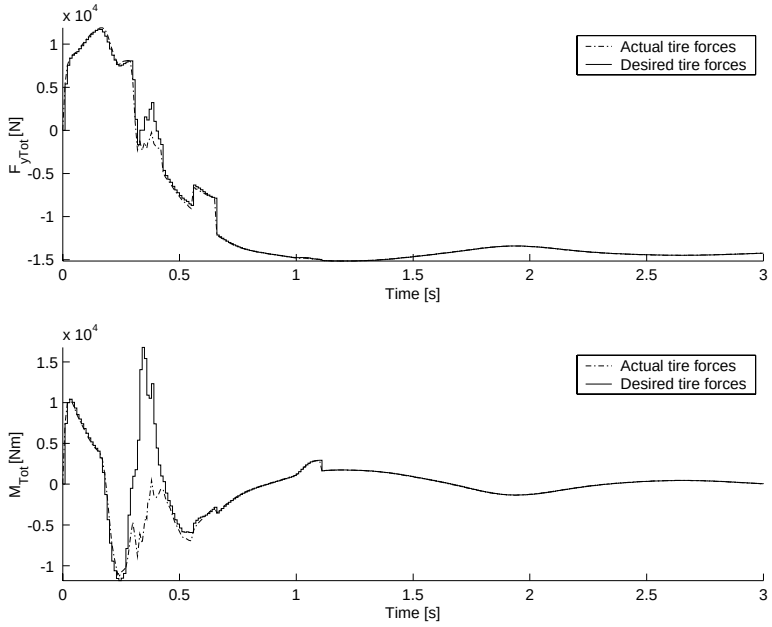

Figure 4.7 The desired and actual tire forces for the nonlinear nonconvex ap proach control allocator.

Linear Approximation

The desired tire forces compared with the actual tire forces are shown in Figure 4.9. The control signals are shown in Figure 4.10. The linear approximation is considerably faster than the other two. But there is no guarantee that the solution found is within the given constraints nor op timal. The approach can also give oscillations in the control signals, see F_{x2R} in Figure 4.10.

Convex Approximation

The desired tire forces compared with the actual tire forces are shown in Figure 4.11. The control signals are shown in Figure 4.12. The solution to the optimization problem was always on the ellipse in the cases tested. Thus, there was no need to adjust ζ, and only one run of the algorithm was necessary. This is interesting, and maybe it is possible to find some theoretical results that explains why.

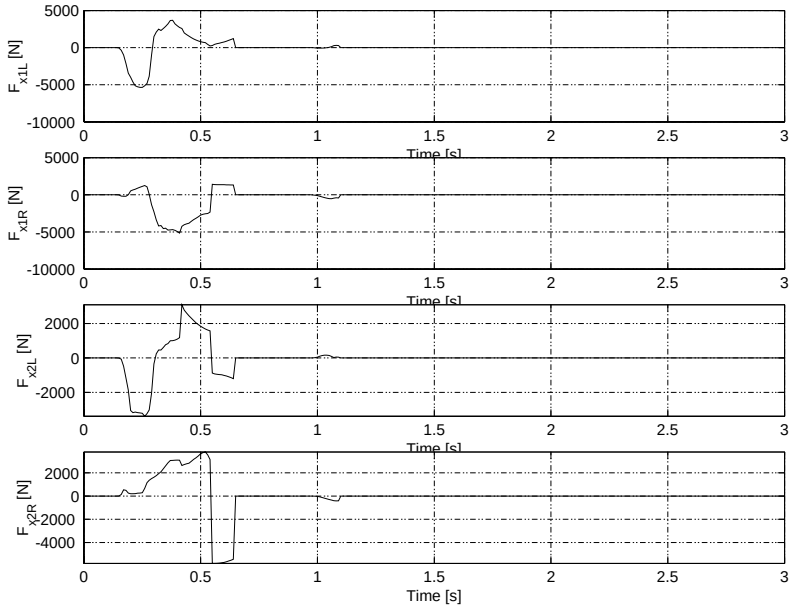

Figure 4.8 The control signals (F_{x1L}, F_{x1R}, F_{x2L}, F_{x2R}) for the nonlinear approach control allocator.

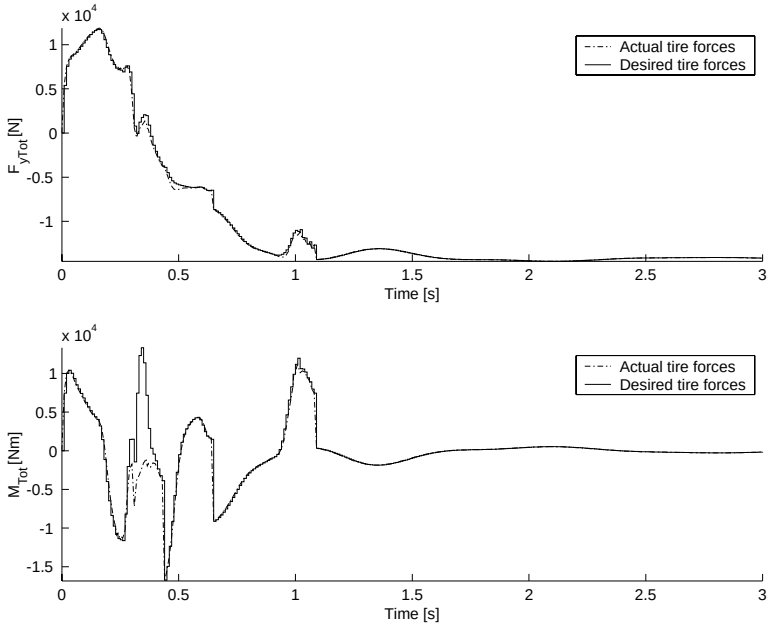

Figure 4.9 The desired and actual tire forces for the linear approximation control allocator.

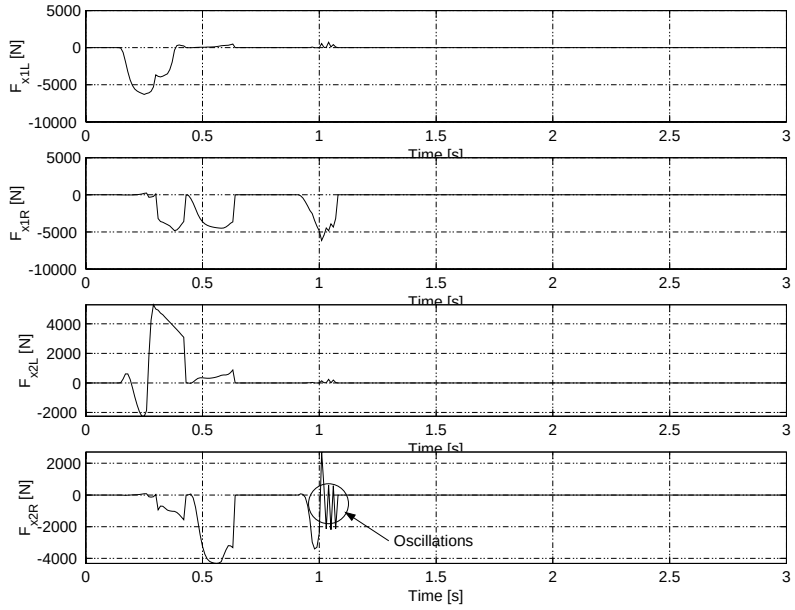

Figure 4.10 The control signals (F_{x1L}, F_{x1R}, F_{x2L}, F_{x2R}) for the linear approxi mation control allocator.

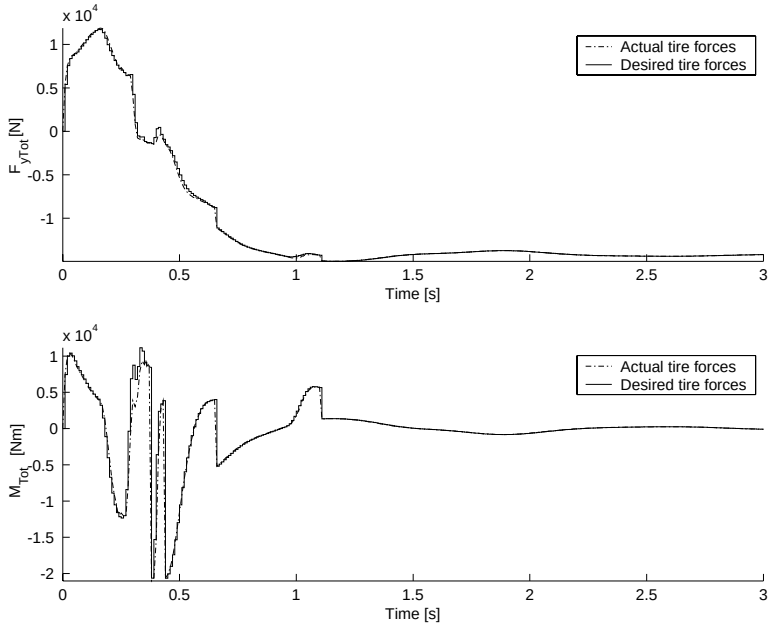

Figure 4.11 The desired and actual tire forces for the convex approximation control allocator.

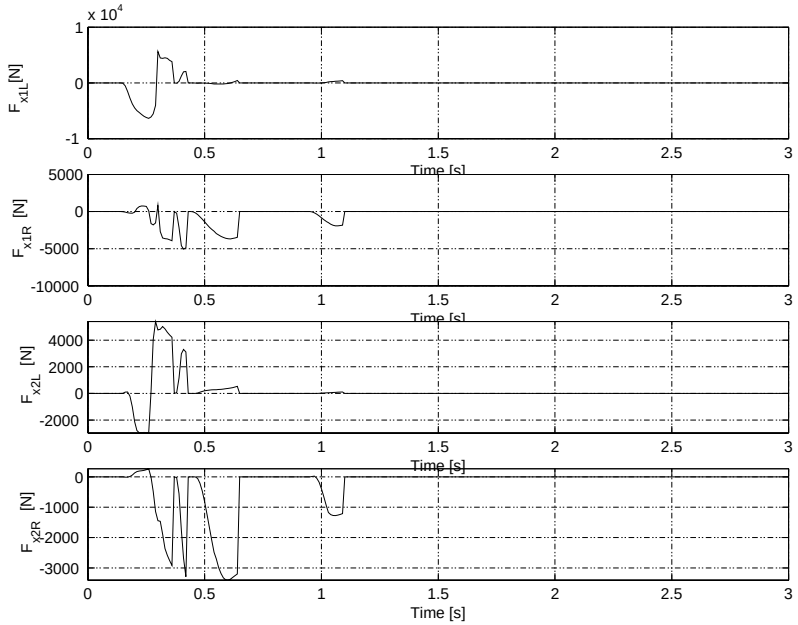

Figure 4.12 The control signals (F_{x1L}, F_{x1R}, F_{x2L}, F_{x2R}) for the convex approxi mation control allocator.

4.6 Total Controller

The convex approximation is considered to be the most reliable of the three control allocators, and it was used to evaluate the performance of the to tal controller. The Road Edge Recovery maneuver were tested with and without the controller activated, and the results with the controller active are presented in Figure 4.13 and Figure 4.14. When the controller was active, no wheel lift off occurred. Compare this with the results without the controller active, Figure 4.15 and Figure 4.16. When the controller is not active, it can clearly be seen that wheel lift off takes place. The control signals when the controller is active are shown in Figure 4.12, and the desired and actual tire forces are shown in Figure 4.11.

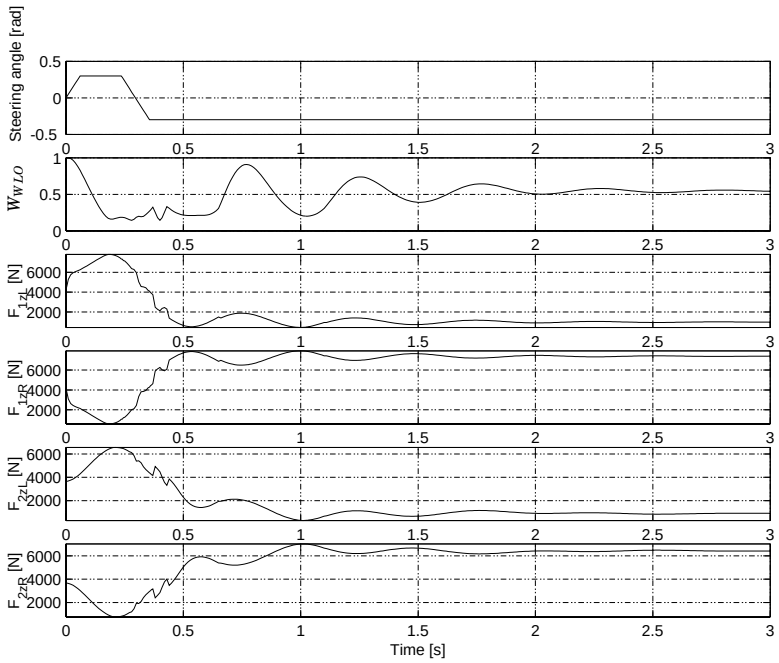

Figure 4.13 The normal forces of the car, the wheel lift off warning signal, and the steering angle during the Road Edge Recovery maneuver with the controller active.

The trajectories of the car without controller and the car with controller are shown in Figure 4.17. The car with the controller do not skid as much as the car without the controller. The difference between the two trajectories are not that large.

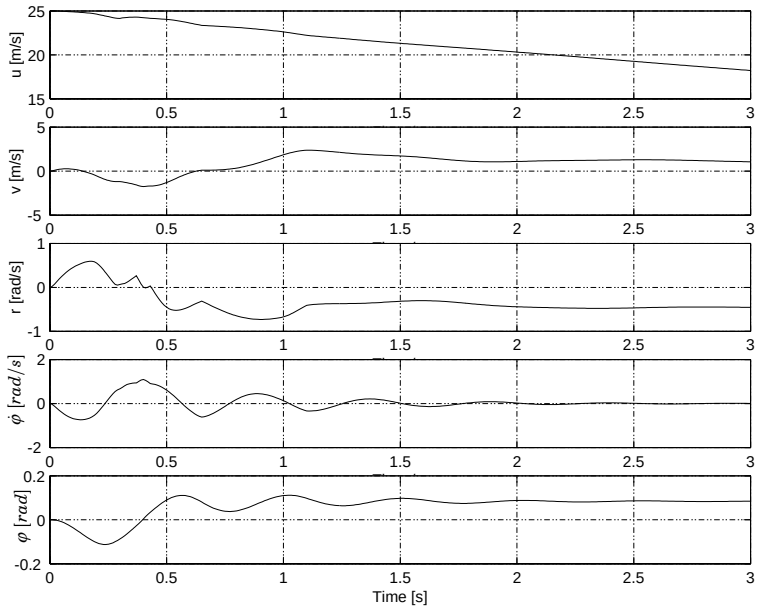

Figure 4.14 The states of the car during the Road Edge Recovery maneuver with the controller active.

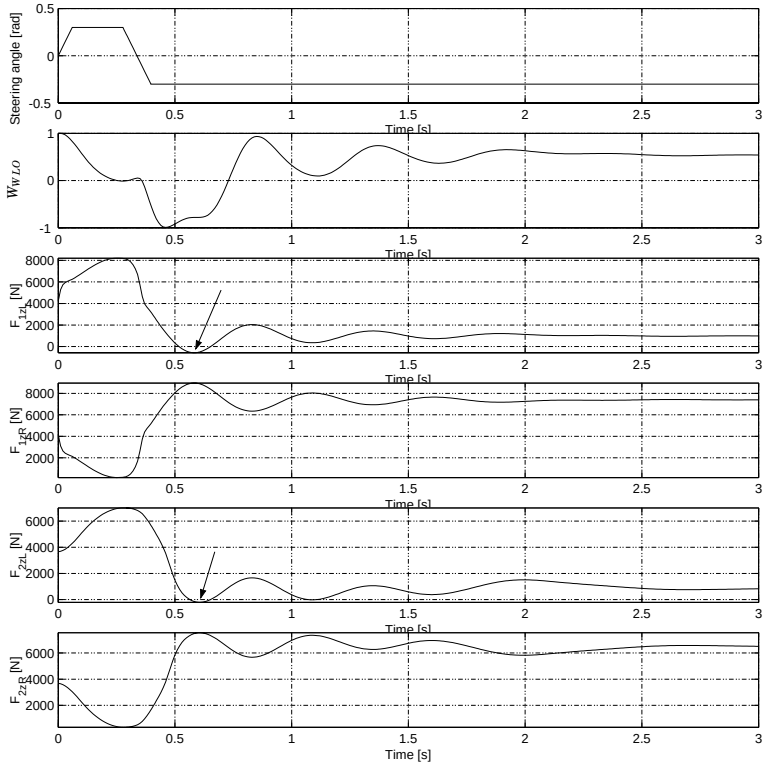

Figure 4.15 The normal forces of the car, the wheel lift off warning signal, and the steering angle during the Road Edge Recovery maneuver without the controller active.

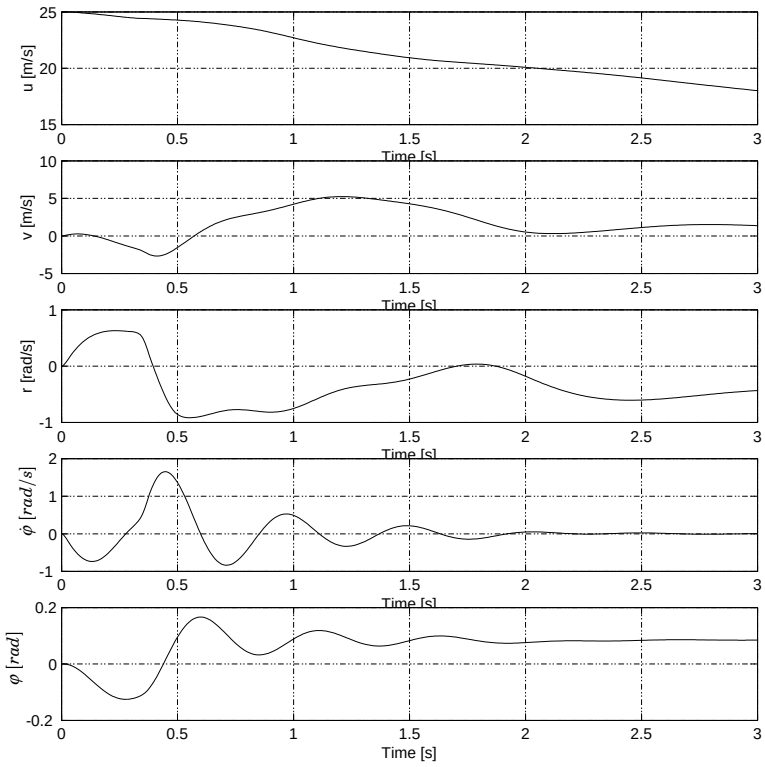

Figure 4.16 The states of the car during the Road Edge Recovery maneuver without the controller active.

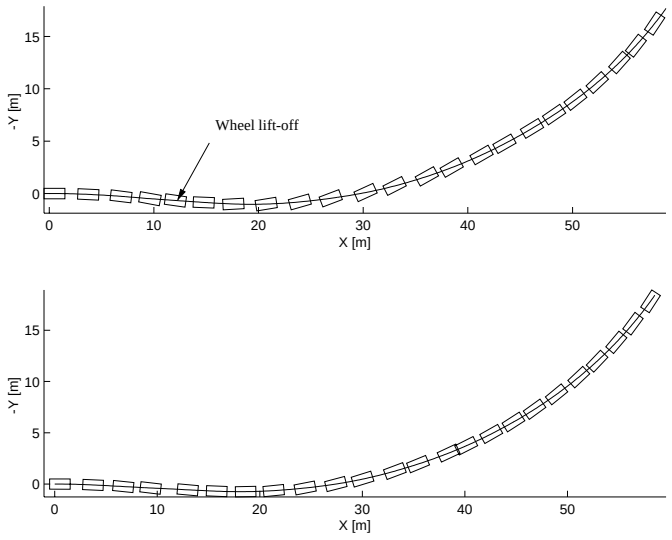

Figure 4.17 *Top* The trajectory of the car without controller. *Bottom* The trajectory of the car with controller.

5. Discussion

The simulations show that the control system can prevent rollover. Thus, the most important objective has been accomplished.

5.1 Rollover Detection

The simulations made, show that the wheel lift off warning signal, W_{WLO}, can be used as a warning signal for wheel lift off. The difference between the transient case and the steady state case is small. The steady state case is easier to calculate, and if simplicity is a factor, then the steady state measure should be used. However, the difference depend on the used vehicle parameters, and the difference can be larger than in the example vehicle used.

The wheel lift off warning signal worked well for transient maneuvers, but simulations have shown that quasi steady state maneuvers can induce wheel lift off without giving a clear and early warning signal. This is a drawback, but it can be compensated with a lower threshold for W_{WLO}, i.e., the controller is more sensitive.

The calculated energies for W_{WLO} are small compared to the energies needed for a complete rollover. This is expected since the W_{WLO} is designed to give a warning signal when wheel lift off is imminent. The W_{WLO} energy is also small compared to the total kinetic energy of the vehicle. But the forward kinetic energy has to be converted into roll kinetic energy before the vehicle perform a rollover. Tripped rollovers are therefore much more likely to occur, since in that case large amounts of kinetic energy can be transformed into roll kinetic energy when the vehicle hits an obstacle.

The force needed to charge the mass spring system with the somewhat small critical energy is quite large. This amount of force is only induced during extreme maneuvers. The critical energy is on the same scale as the kinetic roll energy available during the Road Edge Recovery maneuver, see Table 3.1 and Figure 3.5. These arguments support the plausibility of the measure, despite the fact that the critical energy is small.

5.2 Rollover Prevention

As mentioned before, the most important objective is accomplished. The Road Edge Recovery maneuver does not give a wheel lift off with the con troller activated. This is of course no guarantee that other maneuvers will not induce wheel lift off or rollover.

The validity of the simulation can of course be discussed. The tire model is valid in steady state situations, and the scenarios tested are clearly transient. Furthermore, the tires do not produce forces directly, there is a lag effect that was not included in the used model.

The assumption that the vehicle can apply both forward and backward forces can also be discussed. A more realistic assumption is that only the brakes can be used as fast actuators. Driving torque can also be controlled,

but it is much slower than the brakes. A control allocation approach for braking only is presented in the Future Work section.

Control Allocation

The nonlinear nonconvex control allocation approach does not have to give a globally optimal[1] solution. The method's execution time is also quite unpredictable. This make it a less viable option.

The linear control allocation approach does not have to give an optimal solution either. The execution time is very fast, which is important in real time applications. The method exhibits oscillations, which is undesired. The effect on the chassis will approximately be the same, but there will be much strain and tear on the actuators. It was possible to reduce the oscillations by restricting the control signal more than actually needed, in order to avoid the areas where the derivatives are large. However, oscillations could still be observed.

The convex optimization approach will give an optimal solution, but fixed bounds for the execution time are not available. Since the controller will be used in a real time environment, timing is crucial. The lack of fixed execution time bounds is therefore a drawback, but the method is still considered to be the best solution.

Fine Tuning

The system can probably be more fine tuned to increase the performance. There are a lot of parameters to change. This is both a strength and a weakness. The complexity of the controller makes it capable of performing complicated tasks, and it can be extended to do more. The complexity also makes it possible to adapt the controller to work well on very different vehicle types. The drawback is that complex system usually have a lot of bugs, and it is time consuming to design and maintain. Highly complex systems are usually also less robust than simple systems.

[1]Optimal in the sense that the solution minimizes the used goal function. If this goal function will give the optimal solution in a wider sense is naturally a slightly trickier question

6. Future Work

As mentioned in the introduction, it is essential to have a working observer. To find an observer is the most important future work.

The model used in the simulation has a great drawback, wheel lift off and rollover is not correctly modeled. A better model incorporating this effect is needed. The chassis equations can quite easily be modified to take the changed roll axis into account. It is probably more difficult to find a valid tire model, since not much testing have been performed in these extreme situations.

The testing was only performed with open loop steering angle changes, i.e., the steering angle was controlled according to a fixed program. The controller performance can radically change when there is a closed loop driver controlling the steering angle. More testing with a driver model is needed. The difficulty is to find a simple and accurate driver model.

If simulations with a better vehicle model and driver model are satis factory, then real testing should be done with real SUVs. This is needed in order to validate the results.

The proposed convex approximation for the control allocator does not have a fixed execution time, and it is rather slow. This has to be changed if the algorithm is going to be used in a real time system. Thus, fixed bounds for the amount of needed iterations are needed, and the algorithm/code need to be fine tuned to be faster. It would also be interesting to know under what conditions a solution can be found on the ellipse when $Ax = U$.

If only the brakes are used as actuators, then it is possible to make a convex approximation that is on the ellipse in the best case, and a linear approximation in the worst case. The constraints should be

$$\left(\frac{F_{yi}}{F_{ymax}(\alpha_i, F_{zi})}\right)^2 + \left(\frac{F_{xi}}{\mu F_{zi}}\right)^2 \leq 1$$

$$F_{yi} F_{ymax}(\alpha_i, F_{zi}) \geq 0$$

$$F_{xi} \leq -\mu F_{zi} + F_{yi} \frac{F_{yimax}}{\mu F_{zi}}$$

$$i = \text{ 1L, 1R, 2L, 2R}$$

The first two conditions are used in the already evaluated convex approx imation approach, but the third condition is new. This extra condition will force the solution to be close to the boundary. The new convex set is visu alized in Figure 6.1.

The controller could be extended to perform ESP tasks, when a rollover is out of reach. This should be possible since the proposed controller frame work is flexible, and the control allocator could be used to allocate the forces required by the ESP functions.

If the vehicle have a steer by wire system then the control system can control the steering angle. Then, the influence panic steering maneuvers have on the vehicle dynamics, could maybe be reduced with some sort of low pass filtering of the steering signal.

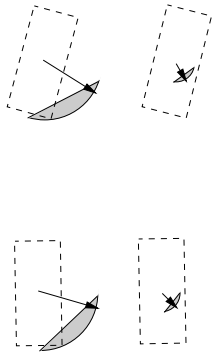

Figure 6.1 Available forces with a limited convex approximation, only using brak ing action.

7. Bibliography

Ackermann, J., Bünte, T. & Odenthal, D. (1999), Advantages of active steering, *in* 'International Symposium on Automotive Technology and Automation'.

Bakker, E., Pacejka, H. B. & Lidner, L. (1989), A new tire model with an application in vehicle dynamics studies, Technical Report 890087, SAE, Society of Automotive Engineers.

Best, M. C. & Gordon, T. J. (1998), Real time state estimation of vehicle handling dynamics using an adaptive kalman filter, *in* 'International Symposium on Advanced Vehicle Control'.

Boyd, S. & Vandenberghe, L. (2004), *Convex Optimization*, Cambridge University Press.

Dahlberg, E. (2001), Commercial Vehicle Stability Focusing on Rollover, PhD thesis, Royal Institute of Technology, Stockholm, Sweden.

Forkenbrock, G. J., O'Harra, B. C. & Elsasser, D. (2003), An experimental examination of 26 light vehicles using test maneuvers that may induce on road, untripped rollover and a discussion of NHTSA's refined test procedures, Technical Report DOT HS 809 547, National Highway Traffic Safety Administration, Vehicle Research and Test Center, P.O. Box 37, East Liberty, OH 43319, USA.

Gillespie, T. D. (1992), *Fundamentals of Vehicle Dynamics*, SAE, Society of Automotive Engineers.

Heydinger, G. J., Bixel, R. A., Garrot, W. R., Pyne, M., Howe, J. G. & Guenther, D. A. (1999), Measured Vehicle Inertial Parameters NHTSA's Data Through November 1998, Technical Report 1999 01 1336, SAE, Society of Automotive Engineers.

Howe, J. G., Garrott, W. R., G. Forkenbrock, G. J. H. & Lloyd, J. (2001), An experimental examination of selected maneuvers that may induce on road, untripped light vehicle rollover, Technical Report DOT HS 809 357, National Highway Traffic Safety Administration, Vehicle Research and Test Center, P.O. Box 37, East Liberty, OH 43319, USA.

Härkegård, O. (2003), Backstepping and Control Allocation with Applica tions to Flight Control, PhD thesis, Department of Electrical Engi neering, Linköping University, Linköping, Sweden.

Matlab on line documentation (n.d.). `http://www.mathworks.com/`.

Odenthal, D., Bünte, T. & Ackermann, J. (1999), Nonlinear steering and braking control for vehicle rollover avoidance, *in* 'Proceedings ECC'99'.

Pacejka, H. B. (2002), *Tyre and Vehicle Dynamics*, Butterworth Heinemann.

Åström, K. J. & Wittenmark, B. (1995), *Adaptive Control*, Addison Wesley.

Åström, K. J. & Wittenmark, B. (1997), *Computer Controlled Systems*, Prentice Hall.

van Zanten, A. T., Erhardt, R., Pfaff, G., Kost, F., Hartmann, U. & Ehret, T. (1996), Control aspects of the Bosch VDC, *in* 'International Symposium on Advanced Vehicle Control'.

Wong, J. Y. (2001), *Theory of Ground Vehicles*, John Wiley & Sons.

A. Appendices

A.1 Vehicle Parameters

Table A.1 The vehicle parameters.

Name	Explanation	Value
m	mass (kg)	1600
h'	Distance from roll axis to CG $[m]$	0.4 & 0.2
a	Distance from front to CG $[m]$	1.4
b	Distance from rear to CG $[m]$	1.6
Θ_r	Angle between roll axis and the XY plane $[rad]$	0.1
I_z	Moment of inertia about the z axis $[kgm^2]$	2300
I_y	Moment of inertia about the y axis $[kgm^2]$	500
I_x	Moment of inertia about the x axis $[kgm^2]$	500
I_{xz}	Product of inertia about the x z axes $[kgm^2]$	100
$k_{\varphi i}$	Roll damping, axle i, i=1,2 $[Ns/rad]$	800
$c_{\varphi i}$	Roll stiffness, axle i, i=1,2 $[N/rad]$	37000
V	Initial forward velocity in the test cases $[m/s]$	25
l	Half length of the wheel axle [m]	1
h	Height from the ground to the roll axis [m]	0.4

The vehicle parameters were extrapolated using Best & Gordon (1998) and Heydinger et al. (1999). The tire parameters were found in Pacejka (2002).

Table A.2 The tire parameters.

Name	Explanation	Value
$B = \frac{C_{F\alpha}}{CD}$	Stiffness factor	Dynamic
C	Shape factor	1.3
$D = \mu F_z$	Peak factor	Dynamic
E	Curvature factor	3
$C_{F\alpha} =$ $c_1 \sin(2 \arctan(\frac{F_z}{c_2}))$	Cornering stiffness	Dynamic
c_1	Maximum cornering stiffness	60000
c_2	Load at max. cornering stiffness	4000

A.2 Penalty Matrices

Q and R are used in the cost function as follows

$$J = E\ \sum_{k=0}^{N-1} (X^T(kh)QX(kh) + U^T(kh)RU(kh)$$

$$Q = \begin{pmatrix} 1 & 0 & 0 & 0 & 0 \\ 0 & 1 & 0 & 0 & 0 \\ 0 & 0 & 1 & 0 & 0 \\ 0 & 0 & 0 & \frac{1}{10000} & 0 \\ 0 & 0 & 0 & 0 & 10000000 \end{pmatrix}$$

Where $X = (u\, v\, r\, \dot{\varphi}\, \varphi)^T$ and $U = (F_y\, F_x\, M)^T$. There is a big scale difference between the elements in Q. This make sense since roll is on another scale than u and v. The scaling factor is typically 100, which means 10000 when squared. The penalty on $\dot{\varphi}$ is chosen to be really small, in order to make φ more movable.

$$R = \begin{pmatrix} \frac{1}{1000} & 0 & 0 \\ 0 & \frac{1}{10000} & 0 \\ 0 & 0 & \frac{1}{1000} \end{pmatrix}$$

A.3 Linearization Points

Table A.3 Linearization points, $u = 25$ m/s

$u = 25$ m/s	Left Turn	Straight Ahead	Right Turn
u	25.0	25.0	25.0
v	2.3	0	-2.3
r	-0.37	0	0.37
$\dot{\varphi}$	-6.9×10^{-22}	0	2.7×10^{-25}
φ	0.087	0	-0.087
δ	-0.20	0	0.20
F_{yTot}	-2.5×10^{-29}	0	8.4×10^{-24}
F_{xTot}	3000.0	0	3000.0
M_{Tot}	-2.5×10^{-29}	0	-8.4×10^{-24}

Table A.4 Linearization points, $u = 17.5$ m/s

$u = 17.5$ m/s	Left Turn	Straight Ahead	Right Turn
u	17.5	17.5	17.5
v	1.19	0	-1.19
r	-0.523	0	0.523
$\dot{\varphi}$	1.80×10^{-22}	0	-1.26×10^{-23}
φ	0.0860	0	-0.0860
δ	-0.200	0	0.200
F_{yTot}	-2.58×10^{-26}	0	-7.70×10^{-34}
F_{xTot}	2650.0	0	2650.0
M_{Tot}	-3.76×10^{-37}	0	7.70×10^{-34}

Table A.5 Linearization points, $u = 10$ m/s

$u = 10$ m/s	Left Turn	Straight Ahead	Right Turn
u	10.0	10.0	10.0
v	-0.487	0	0.487
r	-0.629	0	0.629
$\dot{\varphi}$	-1.7×10^{-22}	0	-1.75×10^{-24}
φ	0.0589	0	-0.0589
δ	-0.200	0	0.200
F_{yTot}	0	0	-7.44×10^{-21}
F_{xTot}	604.0	0	604.0
M_{Tot}	-3.1×10^{-36}	0	3.31×10^{-24}